

World Journal of *Stem Cells*

World J Stem Cells 2020 March 26; 12(3): 168-240



**OPINION REVIEW**

- 168** Mesenchymal stem cells in neurodegenerative diseases: Opinion review on ethical dilemmas
Scopetti M, Santurro A, Gatto V, La Russa R, Manetti F, D'Errico S, Frati P, Fineschi V

REVIEW

- 178** Mesenchymal stem cell-derived extracellular vesicles as a new therapeutic strategy for ocular diseases
Yu B, Li XR, Zhang XM
- 188** Gut commensal bacteria, Paneth cells and their relations to radiation enteropathy
Gao YL, Shao LH, Dong LH, Chang PY

ORIGINAL ARTICLE**Basic Study**

- 203** Efficient differentiation of vascular smooth muscle cells from Wharton's Jelly mesenchymal stromal cells using human platelet lysate: A potential cell source for small blood vessel engineering
Mallis P, Papapanagiotou A, Katsimpoulas M, Kostakis A, Siasos G, Kassi E, Stavropoulos-Giokas C, Michalopoulos E
- 222** CR6-interacting factor-1 contributes to osteoclastogenesis by inducing receptor activator of nuclear factor κ B ligand after radiation
Xiang LX, Ran Q, Chen L, Xiang Y, Li FJ, Zhang XM, Xiao YN, Zou LY, Zhong JF, Li SC, Li ZJ

ABOUT COVER

Editorial Board Member of *World Journal of Stem Cells*, Sujeong Jang, PhD, Assistant Professor, Physiology, Chonnam National University Medical School, Hwasun-gun 58128, South Korea

AIMS AND SCOPE

The primary aim of *World Journal of Stem Cells* (*WJSC*, *World J Stem Cells*) is to provide scholars and readers from various fields of stem cells with a platform to publish high-quality basic and clinical research articles and communicate their research findings online.

WJSC publishes articles reporting research results obtained in the field of stem cell biology and regenerative medicine, related to the wide range of stem cells including embryonic stem cells, germline stem cells, tissue-specific stem cells, adult stem cells, mesenchymal stromal cells, induced pluripotent stem cells, embryoid bodies, embryonal carcinoma stem cells, hemangioblasts, hematopoietic stem cells, lymphoid progenitor cells, myeloid progenitor cells, *etc.*

INDEXING/ABSTRACTING

The *WJSC* is now indexed in PubMed, PubMed Central, Science Citation Index Expanded (also known as SciSearch®), Journal Citation Reports/Science Edition, Biological Abstracts, and BIOSIS Previews. The 2019 Edition of Journal Citation Reports cites the 2018 impact factor for *WJSC* as 3.534 (5-year impact factor: N/A), ranking *WJSC* as 16 among 26 journals in Cell and Tissue Engineering (quartile in category Q3), and 94 among 193 journals in Cell Biology (quartile in category Q2).

RESPONSIBLE EDITORS FOR THIS ISSUE

Responsible Electronic Editor: *Yan-Xia Xing*

Proofing Production Department Director: *Xiang Li*

NAME OF JOURNAL

World Journal of Stem Cells

ISSN

ISSN 1948-0210 (online)

LAUNCH DATE

December 31, 2009

FREQUENCY

Monthly

EDITORS-IN-CHIEF

Tong Cao, Shengwen Calvin Li, Carlo Ventura

EDITORIAL BOARD MEMBERS

<https://www.wjgnet.com/1948-0210/editorialboard.htm>

EDITORIAL OFFICE

Jin-Lei Wang, Director

PUBLICATION DATE

March 26, 2020

COPYRIGHT

© 2020 Baishideng Publishing Group Inc

INSTRUCTIONS TO AUTHORS

<https://www.wjgnet.com/bpg/gerinfo/204>

GUIDELINES FOR ETHICS DOCUMENTS

<https://www.wjgnet.com/bpg/GerInfo/287>

GUIDELINES FOR NON-NATIVE SPEAKERS OF ENGLISH

<https://www.wjgnet.com/bpg/gerinfo/240>

PUBLICATION MISCONDUCT

<https://www.wjgnet.com/bpg/gerinfo/208>

ARTICLE PROCESSING CHARGE

<https://www.wjgnet.com/bpg/gerinfo/242>

STEPS FOR SUBMITTING MANUSCRIPTS

<https://www.wjgnet.com/bpg/GerInfo/239>

ONLINE SUBMISSION

<https://www.f6publishing.com>



Basic Study

CR6-interacting factor-1 contributes to osteoclastogenesis by inducing receptor activator of nuclear factor κ B ligand after radiation

Li-Xin Xiang, Qian Ran, Li Chen, Yang Xiang, Feng-Jie Li, Xiao-Mei Zhang, Yan-Ni Xiao, Ling-Yun Zou, Jiang F Zhong, Shengwen Calvin Li, Zhong-Jun Li

ORCID number: Li-Xin Xiang (0000-0003-1704-829X); Li Chen (0000-0003-1939-9659); Yang Xiang (0000-0003-4015-5464); Feng-Jie Li (0000-0003-0981-5129); Xiao-Mei Zhang (0000-0003-3093-2354); Yan-Ni Xiao (0000-0002-3473-1050); Ling-Yun Zou (0000-0002-1109-5709); Jiang F Zhong (0000-0003-0551-5161); Qian Ran (0000-0003-2855-2598); Shengwen Calvin Li (0000-0002-9699-9204); Zhong-Jun Li (0000-0001-7629-0911).

Author contributions: Li ZJ and Xiang LX conceived the study; Xiang LX designed and performed most experiments and data analysis; Chen L, Xiang Y, Li FJ, Zhang XM, Xiao YN, Zou LY, Zhong JF, Li SC, and Ran Q assisted with experiments and data analysis; Xiang LX wrote and edited the manuscript; Li ZJ supervised the study; all authors read and approved the final manuscript.

Supported by National Natural Science Foundation of China, No. 81502754 and No. 31571352; and Interdisciplinary and International Cooperation Projects of The Second Affiliated Hospital, Third Military Medical University, No. 2016YXKJC0.

Institutional review board statement: Not applicable.

Institutional animal care and use committee statement: All animal studies performed were approved by the Laboratory Animal Welfare and Ethics Committee Of the Third

Li-Xin Xiang, Qian Ran, Li Chen, Yang Xiang, Feng-Jie Li, Xiao-Mei Zhang, Yan-Ni Xiao, Zhong-Jun Li, Laboratory Medicine Center, Department of Blood Transfusion, Lab of Radiation Biology, The Second Affiliated Hospital, Third Military Medical University, Chongqing, 400037, China

Qian Ran, Yang Xiang, Jiang F Zhong, Department of Otolaryngology, Keck School of Medicine, University of Southern California, Los Angeles, CA 90033, United States

Ling-Yun Zou, Bioinformatics Center, College of Basic Medical Sciences, Third Military Medical University, Chongqing 400038, China

Shengwen Calvin Li, CHOC Children's Research Institute, Children's Hospital of Orange County, University of California, Irvine, CA 92688, United States

Corresponding author: Zhong-Jun Li, MD, Professor, Chief, Laboratory Medicine Center, Department of Blood Transfusion, Lab of Radiation Biology, The Second Affiliated Hospital, Third Military Medical University, Xinqiao Road, Chongqing 400037, China. johnneyusc@gmail.com

Abstract

BACKGROUND

Radiation induces rapid bone loss and enhances bone resorption and adipogenesis, leading to an increased risk of bone fracture. There is still a lack of effective preventive or therapeutic method for irradiation-induced bone injury. Receptor activator of nuclear factor κ B ligand (RANKL) provides the crucial signal to induce osteoclast differentiation and plays an important role in bone resorption. However, the mechanisms of radiation-induced osteoporosis are not fully understood.

AIM

To investigate the role of CR6-interacting factor-1 (Crif1) in osteoclastogenesis after radiation and its possible mechanism.

METHODS

C57BL/6 mice were exposed to Co-60 gamma rays and received 5 Gy of whole-body sublethal irradiation at a rate of 0.69 Gy/min. For *in vitro* study, mouse bone marrow mesenchymal stem/stromal cells (BM-MSCs) were irradiated with Co-60 at a single dose of 9 Gy. For osteoclast induction, monocyte-macrophage RAW264.7 cells were cocultured with mouse BM-MSCs for 7 d. ClusPro and InterProSurf were used to investigate the interaction interface in Crif1 and protein kinase cyclic adenosine monophosphate (cAMP)-activated catalytic

Military Medical University.

Conflict-of-interest statement: The authors report no conflicts of interest in this work.

Data sharing statement: No additional data are available.

ARRIVE guidelines statement: The authors have read the ARRIVE guidelines, and the manuscript was prepared and revised according to the ARRIVE guidelines.

Open-Access: This article is an open-access article that was selected by an in-house editor and fully peer-reviewed by external reviewers. It is distributed in accordance with the Creative Commons Attribution NonCommercial (CC BY-NC 4.0) license, which permits others to distribute, remix, adapt, build upon this work non-commercially, and license their derivative works on different terms, provided the original work is properly cited and the use is non-commercial. See: <http://creativecommons.org/licenses/by-nc/4.0/>

Manuscript source: Unsolicited manuscript

Received: January 23, 2020

Peer-review started: January 23, 2020

First decision: February 19, 2020

Revised: March 9, 2020

Accepted: March 15, 2020

Article in press: March 15, 2020

Published online: March 26, 2020

P-Reviewer: Rakhshan V

S-Editor: Tang JZ

L-Editor: Wang TQ

E-Editor: Ma YJ



subunit alpha complex. Virtual screening using 462608 compounds from the Life Chemicals database around His120 of Crif1 was carried out using the program Autodock_vina. A tetrazolium salt (WST-8) assay was carried out to study the toxicity of compounds to different cells, including human BM-MSCs, mouse BM-MSCs, and Vero cells.

RESULTS

Crif1 expression increased in bone marrow cells after radiation in mice. Overexpression of Crif1 in mouse BM-MSCs and radiation exposure could increase RANKL secretion and promote osteoclastogenesis *in vitro*. Deletion of Crif1 in BM-MSCs could reduce both adipogenesis and RANKL expression, resulting in the inhibition of osteoclastogenesis. Deletion of Crif1 in RAW264.7 cells did not affect the receptor activator of nuclear factor κ B expression or osteoclast differentiation. Following treatment with protein kinase A (PKA) agonist (forskolin) and inhibitor (H-89) in mouse BM-MSCs, Crif1 induced RANKL secretion *via* the cAMP/PKA pathway. Moreover, we identified the Crif1-protein kinase cyclic adenosine monophosphate-activated catalytic subunit alpha interaction interface by *in silico* studies and shortlisted interface inhibitors through virtual screening on Crif1. Five compounds dramatically suppressed RANKL secretion and adipogenesis by inhibiting the cAMP/PKA pathway.

CONCLUSION

Crif1 promotes RANKL expression *via* the cAMP/PKA pathway, which induces osteoclastogenesis by binding to receptor activator of nuclear factor κ B on monocytes-macrophages in the mouse model. These results suggest a role for Crif1 in modulating osteoclastogenesis and provide insights into potential therapeutic strategies targeting the balance between osteogenesis and adipogenesis for radiation-induced bone injury.

Key words: Irradiation; Osteoporosis; Bone marrow; Mesenchymal stem cells; Monocyte macrophage; Bone

©The Author(s) 2020. Published by Baishideng Publishing Group Inc. All rights reserved.

Core tip: Current treatment of osteoporosis is based mainly on inhibiting bone resorption or stimulating bone generation to increase bone mass; however, the side-effects of some drugs affect long-term administration and adherence. There is still a lack of effective preventive or therapeutic method for radiation-induced bone injury. Because of the contribution of adipocytes to osteoporosis, future drug screening should target not only the regulation of the balance between bone formation and bone resorption but also the balance between osteogenic and adipogenic differentiation. Here, through screening, we identified five CR6-interacting factor-1 inhibitors targeting CR6-interacting factor-1-protein kinase cyclic adenosine monophosphate-activated catalytic subunit alpha interaction interface that could dramatically reduce receptor activator of nuclear factor κ B ligand secretion and adipogenesis. Our study provides insights into potential therapeutic strategies for radiation-induced bone injury.

Citation: Xiang LX, Ran Q, Chen L, Xiang Y, Li FJ, Zhang XM, Xiao YN, Zou LY, Zhong JF, Li SC, Li ZJ. CR6-interacting factor-1 contributes to osteoclastogenesis by inducing receptor activator of nuclear factor κ B ligand after radiation. *World J Stem Cells* 2020; 12(3): 222-240

URL: <https://www.wjgnet.com/1948-0210/full/v12/i3/222.htm>

DOI: <https://dx.doi.org/10.4252/wjsc.v12.i3.222>

INTRODUCTION

Exposure to radiation, such as accident or terrorism, radiotherapy for cancer, and astronauts on exploratory missions beyond low-Earth orbit, can cause rapid bone loss and increase the risk of bone fracture^[1,2]. The risk of a hip fracture for women receiving pelvic irradiation for the treatment of carcinomas of the cervix or rectum is

three times as much as that of the population of women who do not receive radiotherapy^[3]. Osteoporosis is often a long-term complication of radiotherapy, which is characterized by an imbalance in skeletal turnover with reduced bone formation and enhanced bone resorption^[4]. Current treatment of osteoporosis is based mainly on inhibiting bone resorption or stimulating bone generation to increase bone mass; however, the side-effects of some drugs affect long-term administration and adherence. There is still a lack of effective preventive or therapeutic method for irradiation-induced bone injury^[5].

Bone homeostasis is maintained by various types of cells, such as osteoblasts and osteoclasts, which are differentiated from different stem cells in the bone marrow. Osteoblasts are the bone-forming cells derived from bone marrow mesenchymal stem/stromal cells (BM-MSCs) and play an important role in the regulation of bone mass^[6]. Meanwhile, osteoclasts are large, multinucleated cells derived from haematopoietic progenitors of the monocyte-macrophage lineage. Osteoclasts are the principal cells capable of resorbing bone and play an essential role in bone remodeling^[7]. The differentiation of osteoclast is mainly regulated by macrophage colony-stimulating factor, receptor activator of nuclear factor κ B ligand (RANKL), and osteoprotegerin (OPG). Macrophage colony-stimulating factor is required for the survival and proliferation of osteoclast precursors, but RANKL and OPG play central roles in the activation of osteoclastogenesis^[8]. By binding to receptor activator of nuclear factor κ B (RANK) (on haematopoietic progenitors), RANKL provides the crucial signal to induce osteoclast differentiation from haematopoietic progenitor cells as well as to activate mature osteoclasts. OPG is a soluble decoy receptor that can bind to RANKL and negatively regulate RANKL binding to RANK^[9]. BM-MSCs, osteocytes, osteoblasts, adipocytes, and activated T and B lymphocytes are the main sources of RANKL secretion. RANKL expression is promoted by radiation, inflammation, cytokines, hormones, and a number of other agents, including those that signal through protein kinase A (PKA), glycoprotein 130, and vitamin D receptor^[10,11]. Following radiation exposure, BM-MSCs appear to preferentially differentiate into adipocytes instead of osteoblasts, which results in a reduction of bone formation and an increase in bone marrow fat accumulation^[12,13]. And the irradiation-induced bone loss is also associated with increased osteoclast numbers and resorbing surfaces of osteoclasts lining trabeculae^[14]. However, the molecular mechanisms of cell fate decisions in the differentiations of BM-MSCs and osteoclasts involved in irradiation-induced bone loss are still not fully understood.

CR6-interacting factor-1 (Crif1) is a multifunctional protein that can interact with many proteins to induce cell cycle arrest, modulate oxidative stress and cell radiosensitivity, and regulate transcriptional activity through interactions with the DNA-binding domains of transcription factors^[15-21]. It is also the constitutive protein of the large mitoribosomal subunit required for the synthesis and insertion of mitochondrial-encoded OxPhos polypeptides into the mitochondrial membrane^[22]. Crif1 deficiency in macrophages impairs mitochondrial oxidative function and causes systemic insulin resistance and adipose tissue inflammation^[23]. Our previous study showed that Crif1 promotes adipogenic differentiation of BM-MSCs after radiation by modulating the cyclic adenosine monophosphate (cAMP)/PKA signaling pathway^[24].

In this study, we investigated the role of Crif1 in osteoclastogenesis after radiation. Here, we showed that *Crif1* deletion caused decreases in RANKL expression and the RANKL/OPG ratio and reduced osteoclastogenesis and adipogenesis after radiation. Through screening, we also identified five compounds that could effectively inhibit RANKL expression and adipogenesis. We demonstrated that Crif1 promoted osteoclastogenesis by inducing RANKL expression *via* the cAMP/PKA pathway. Our study suggests a role for Crif1 in modulating osteoclastogenesis and provides insights into potential therapeutic strategies targeting the balance between osteogenesis and adipogenesis for radiation-induced bone injury.

MATERIALS AND METHODS

Animals

The animal protocol was designed to minimize pain or discomfort to the animals. All animal studies performed were approved by the Laboratory Animal Welfare and Ethics Committee Of the Third Military Medical University. C57BL/6 mice (aged 12-14 wk) were purchased from Beijing HFK Bio-Technology Co. Ltd. Mice were maintained under specific pathogen-free conditions and fed standard mouse chow and water. For radiation treatment, mice ($n = 6$ /group) were exposed to Co-60 gamma rays and received 5 Gy of whole-body sublethal irradiation at a rate of 0.69 Gy/min.

Cell culture and treatment

For *in vitro* study, mouse BM-MSCs purchased from Cyagen Biosciences were cultured in mouse mesenchymal stem cell medium (MUCMX-90011, Cyagen Biosciences) at 37 °C in an atmosphere containing 5% CO₂.

For radiation treatment, mouse BM-MSCs were irradiated with a single dose of 9 Gy Co-60 at a rate of 0.69 Gy/min. RAW264.7 cells were cultured in Dulbecco's modified Eagle medium (HyClone) supplemented with 10% fetal bovine serum.

For osteoclast induction, RAW264.7 cells (2×10^4 /well) seeded in the upper well and mouse BM-MSCs (5×10^4 /well) seeded in the lower well of a 12-well transwell unit (0.4 µm) were cocultured for 7 d with or without forskolin (25 µmol/L) or H-89 (20 µmol/L) treatment. After 7 d of coculture, cells were collected for real-time quantitative polymerase chain reaction (RT-qPCR) and Western blot analysis; meanwhile, the supernatant medium was collected for enzyme linked immunosorbent assay (ELISA).

Human bone marrow mesenchymal stem/stromal cells (H-BM-MSCs) (catalogue No. 7500, ScienCell) were cultured in mesenchymal stem cell medium (catalogue No. 7501, ScienCell) at 37 °C in an atmosphere containing 5% CO₂.

Micro-computed tomography analysis

Femurs were dissected, fixed overnight in 4% paraformaldehyde, and stored in 1% paraformaldehyde at 4 °C. Trabecular bone parameters were measured in the distal metaphysis of the femur. We started analysing slices at the bottom of the distal growth plate, where the epiphyseal cap structure completely disappeared, and continued for 95 slices (10.5 µm/slice, using SCANCO VivaCT40) towards the proximal end of the femur.

Isolation of bone marrow cells

Femurs were collected and cleaned in sterile phosphate buffered saline (PBS), and both ends of each femur were trimmed off. Bones were placed in a 0.6-mL microcentrifuge tube that was cut open at the bottom and nestled inside a 1.5-mL microcentrifuge tube. Fresh bone marrow was spun out by brief centrifugation (from 0 rpm to 10000 rpm, 9 s). Red blood cells were lysed using RBC lysis buffer (catalog No. RT122-02, TIANGEN). After centrifugation (3000 rpm, 5 min), cells in the bottom layer were collected for Western blot and RT-qPCR assays.

Crif1 knockout and overexpression *in vitro*

For Crif1 overexpression, mouse BM-MSCs were transfected with a Crif1 lentiviral overexpression vector (pLV[Exp]-EGFP:T2A:Puro-EF1A>mGadd45gip1[NM_183358.4]) constructed by Cyagen Biosciences (vector ID: VB180112-1182ypt) and selected with 5 µg/mL puromycin dihydrochloride (A1113803, Invitrogen). An empty vector (pLV[Exp]-EGFP:T2A:Puro-Null, vector ID: VB160420-1011mqh, Cyagen Biosciences) was included as a control.

For Crif1 knockout, mouse BM-MSCs were first transfected with lentiCas9-Blast vector (Genomeditech) and selected with 5 µg/mL blasticidin S HCl (A1113903, Invitrogen). Then, cells were transfected with CRISPR/Cas9 M_Gadd45gip1 gRNA vector (target sequence: GCGGGGCGCACGGTAGCTG, Genomeditech) and selected with 5 µg/mL puromycin dihydrochloride. An empty vector (LentiGuide-Puro-Scramble-gRNA, Genomeditech) was included as a control.

In vitro adipogenic differentiation

To induce adipogenesis, mouse BM-MSCs were seeded at a density of 2×10^4 cells per well in 6-well plates and cultured in mouse mesenchymal stem cell adipogenic differentiation medium (MUCMX-90031, Cyagen Biosciences). Human BM-MSCs were seeded at a density of 2×10^4 cells per well in 6-well plates and cultured in human mesenchymal stem cell adipogenic differentiation medium (HUXMA-90031, Cyagen Biosciences). After 21 d of differentiation, we preserved the supernatant medium for ELISA and fixed the cells with 2 mL of 4% formaldehyde solution for 30 min. Then, the cells were stained with 1 mL of oil red O working solution (catalog No. S0131, Cyagen Biosciences) for 30 min and visualized under a light microscope (Leica DMIRB, Heidelberg, Germany). The dye from oil red O staining was extracted using isopropanol, and the optical density at 510 nm was measured using a Varioskan FLASH microplate reader.

Western blot analysis and antibodies

Protein expression in the samples was analysed by Western blot. Briefly, total protein lysates were extracted with cell lysis buffer for Western blot and immunoprecipitation (catalog No. P0013, Beyotime) and denatured by boiling. Protein samples were resolved on 12% SDS-polyacrylamide gels and transferred to polyvinylidene fluoride

membranes (Western Blotting Membranes; Roche). Membranes were blocked in PBS containing 5% (w/v) nonfat dry milk and 0.1% Tween 20 and then incubated with the appropriate primary antibodies overnight at 4 °C. Membranes were washed with Tris-buffered saline with Tween-20 three times and then incubated with the appropriate horseradish peroxidase-conjugated secondary antibody for 1 h at 24 °C. Immunoreactive bands were detected with the BeyoECL Plus reagent (P0018, Beyotime) using a Photo-Image System (Molecular Dynamics, Sunnyvale, CA, United States). The primary antibodies used for blotting were as follows: Crif1 (M-222) (sc-134882; Santa Cruz), RANK (H-7) (sc-374360; Santa Cruz), A-FABP (AP2, sc-18661; Santa Cruz), PPAR γ (sc-7273; Santa Cruz), β -actin (sc-47778; Santa Cruz), phospho-cAMP response element-binding protein (CREB) rabbit mAb (#9198; Cell Signaling Technology), and CREB rabbit mAb (#9197; Cell Signaling Technology).

RT-qPCR

RT-qPCR was used to analyze the mRNA levels of selected genes in collected samples. Total RNA was extracted using TRIzol Reagent (catalog No. 10296010, Invitrogen) according to the manufacturer's instructions. First-strand cDNA was synthesized from 1 μ g of RNA using the PrimeScript RT Reagent Kit with gDNA Eraser (catalog No. RR047A, TaKaRa). qPCR was performed in triplicate in 20- μ L reactions containing SYBR Premix Ex Taq II (catalog No. RR820A, TaKaRa). The reaction protocol was as follows: Heating for 30 s at 95 °C, followed by 40 cycles of amplification (5 s at 95 °C and 30 s at 60 °C).

The sequences of the RT-PCR primers are as follows: M-Crif1-F: GAACGCTGGGAGAAAATTCA and M-Crif1-R: ATAGTTCCTGGAAGCGAGCA; M-actin-F: AGCCATGTACGTAGCCATCC and M-actin-R: CTCAGCTGTGGTGGTGAA; M-Rankl-F: GCTCCGAGCTGGTGAAGAAA and M-Rankl-R: CCCCAGAGTACGTGCGCATCT; M-OPG-F: GTTCCTGCACAGCTTCACAA and M-OPG-R: AAACAGCCCAGTGACCATTC.

ELISA

The concentrations of RANKL and OPG were measured using the Mouse RANKL ELISA Kit (E-EL-M0644c, elabscience), Human Soluble Receptor Activator of Nuclear Factor- κ B Ligand ELISA Kit (E-EL-H5558c, elabscience), Mouse OPG ELISA Kit (E-EL-M0081c, elabscience), and Human OPG ELISA Kit (E-EL-H1341c, elabscience) according to the manufacturer's instructions.

Tartrate-resistant acid phosphatase staining

After the 7-d coculture period, cells were washed once with PBS, fixed in 10% formalin for 10 min, and incubated with a substrate solution, naphthol AS-BI phosphate (catalog No. 387, Sigma), in the presence of 50 mmol/L sodium tartrate at 37 °C for 1 h. The resulting mononuclear and multinuclear tartrate-resistant acid phosphatase (TRAP)-positive cells were visualized by light microscopy and quantified.

Histomorphometric analysis

Femurs were dissected, fixed overnight in 4% paraformaldehyde, decalcified in 10% EDTA (pH 7.0) for 20 d, and embedded in paraffin. Longitudinally oriented sections of bone (4 μ m thick), including the metaphysis and diaphysis, were processed for hematoxylin and eosin staining. Dewaxed sections were also stained for TRAP activity to identify osteoclasts. Sections were incubated in TRAP stain for 45 min at 37 °C.

Crif1 inhibitor screening

ClusPro and InterProSurf were used to investigate the interaction interface in Crif1-protein kinase cyclic adenosine monophosphate-activated catalytic subunit alpha (PRKACA) complex. Virtual screening using 462608 compounds from the Life Chemicals database around His¹²⁰ of Crif1 was carried out using the program Autodock_vina. For inhibitor screening, H-BM-MSCs were cultured at a density of 1×10^5 cells per well in 6-well plates and pretreated with five different compounds (25 μ mol/L). After 3 h of pretreatment, forskolin (25 μ mol/L) was added to the medium. After 1 h of forskolin treatment, total protein lysates were extracted for CREB phosphorylation detection, and 3 d later, the supernatant medium was collected for ELISA.

Tetrazolium salt (WST-8) assay

A tetrazolium salt (WST-8) assay was carried out to study the toxicity of compounds to different cells, including human BM-MSCs, mouse BM-MSCs, and Vero cells. Cells seeded at a density of 3000 cells per well in 96-well plates were treated with five

different compounds at eight final concentrations (3.125 $\mu\text{mol/L}$, 6.25 $\mu\text{mol/L}$, 12.5 $\mu\text{mol/L}$, 25 $\mu\text{mol/L}$, 50 $\mu\text{mol/L}$, 100 $\mu\text{mol/L}$, 200 $\mu\text{mol/L}$, and 400 $\mu\text{mol/L}$). Three days later, 10 μL of cell counting kit-8 solution was added to each well. After 4 h of incubation, the absorbance at 450 nm was measured using a Varioskan FLASH microplate reader (Thermo).

Statistical analysis

The mRNA expression levels of *RANKL* and *OPG* in the tested samples were determined as the cycle threshold (CT) level, and normalized copy numbers (relative quantification) were calculated using the $\Delta\Delta\text{CT}$ equation as follows: $-\Delta\Delta\text{CT} = -\Delta\text{CT}$ of the bone marrow sample $-\Delta\text{CT}$ of β -actin, and the normalized copy number (relative quantification) = $2^{-\Delta\Delta\text{CT}}$. The statistical significance of differences between the two groups was assessed using two-tailed Student's *t*-tests. The statistical significance of differences among more than two groups was assessed using one-way ANOVA with Sidak's multiple comparison tests. The statistical significance of differences between radiation treatments in mouse BM-MSCs and *Crif1* knockout BM-MSCs experiments, radiation treatments in mouse BM-MSCs and *Crif1* knockout BM-MSCs adipogenic differentiation experiments, forskolin treatments in mouse BM-MSCs and *Crif1* knockout BM-MSCs experiments, and H-89 treatments in mouse BM-MSCs and *Crif1*-overexpressing BM-MSCs experiments were assessed using two-way ANOVA with Bonferroni's or Sidak's multiple comparison tests. All data are expressed as the mean \pm standard deviation. A *P* value less than or equal to 0.05 was considered statistically significant.

RESULTS

Radiation induces bone loss and increased *Crif1* expression in mice

To confirm the extent of bone loss over the short term after irradiation, we irradiated mice with a single dose of 5 Gy, and then, 7 d later, we harvested the left femurs. Micro-computed tomography analysis of the distal femurs of both males and females at 12 wk of age revealed significant decreases in trabecular bone volume/total volume (Figure 1A and B), connectivity density (Figure 1C), trabecular number (Figure 1D), and bone mineral density (Figure 1E), as well as significant increases in trabecular spacing (Figure 1G) and structure model index (Figure 1H). There was no significant difference in trabecular thickness (Figure 1F). Hematoxylin and eosin staining of femoral sections from irradiated mice showed significantly decreased trabecular bone (Figure 1I), while increased adipocytes (Figure 1J) compared to controls. Paraffin sections of femurs showed more TRAP-positive cells in irradiated mice than in control mice (Figure 1K), indicating the increased number of osteoclasts. These results indicated that radiation-induced adipogenesis and osteoclastogenesis. Moreover, RT-qPCR data revealed dramatic increases in *RANKL* expression (Figure 1L) and the *RANKL*/*OPG* ratio in irradiated bone marrow cells (Figure 1M). *OPG* expression was not affected by radiation treatment (Figure 1L). Notably, expression of *Crif1* also increased in irradiated bone marrow cells compared with control cells 7 d after irradiation (Figure 1N and O).

Overexpression of *Crif1* in BM-MSCs increases *RANKL* secretion and osteoclastogenesis

BM-MSCs are thought to be more resistant to radiation compared with other cells in the bone marrow, such as hematopoietic stem cells and T and B lymphocytes^[25]. Moreover, BM-MSCs are the progenitors of bone marrow osteoblasts and adipocytes^[26]. To investigate the role of *Crif1* in osteoclastogenesis *in vitro*, we transfected mouse BM-MSCs with a *Crif1* lentiviral overexpression vector (Figure 2A). For osteoclast induction *in vitro*, *Crif1*-overexpressing BM-MSCs and RAW264.7 cells were cocultured in a 12-well transwell unit for 7 d. RT-qPCR results showed that the relative mRNA expression of *RANKL* and *RANKL*/*OPG* ratio both increased in *Crif1*-overexpressing BM-MSCs compared to controls after 7 d of coculture (Figure 2B and C). Concentrations of *RANKL* and *OPG* in coculture medium were also detected by ELISA. *Crif1*-overexpressing BM-MSCs produced high levels of *RANKL* compared to the control (Figure 2D), while there was no significant difference in *OPG* concentration between the two groups (Figure 2E). The *RANKL*/*OPG* ratio in *Crif1*-overexpressing BM-MSCs was higher than that in the control (Figure 2F). We also detected an increased number of TRAP-positive cells in RAW264.7 cells cocultured with *Crif1*-overexpressing BM-MSCs (Figure 2G and H). These data suggested that *Crif1* could promote *RANKL* expression and may be involved in osteoclast differentiation.

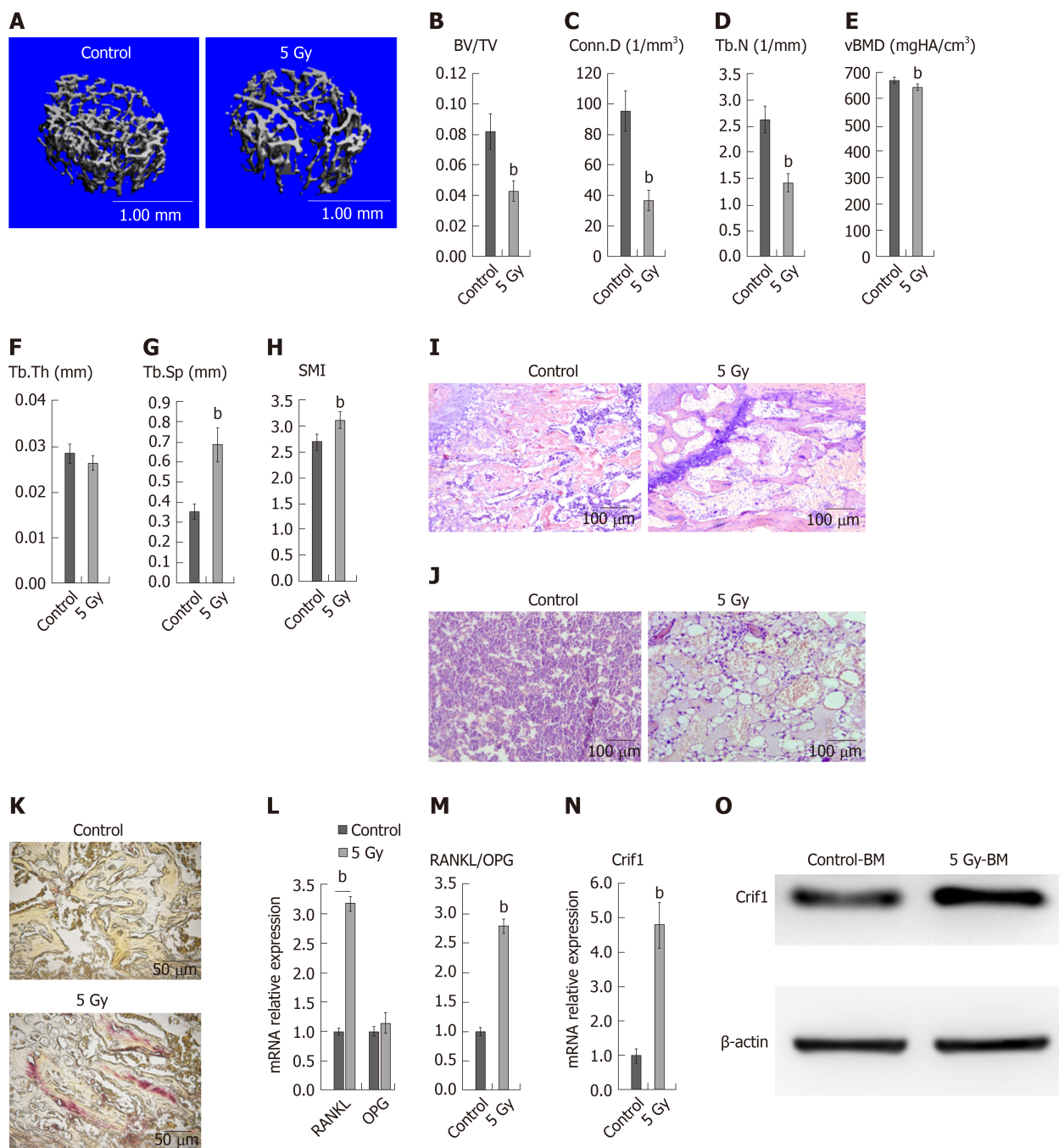


Figure 1 Radiation induces bone loss and increased CR6-interacting factor-1 expression in mice. A: Micro-computed tomography images of the distal metaphysis of the femur. Mice ($n = 6/\text{group}$) were exposed to Co-60 gamma rays, and received 5 Gy of whole-body sublethal irradiation at a rate of 0.69 Gy/min; B-H: Micro-computed tomography analysis of the trabecular bone volume/total volume (B), connectivity density (C), trabecular number (D), bone mineral density (E), trabecular thickness (F), trabecular spacing (G), and structure model index (H); I: Hematoxylin-eosin staining of femoral sections from irradiated mice and controls. Femoral sections from irradiated mice showed significantly decreased trabecular bone compared to controls; J: Hematoxylin-eosin staining of femoral sections from irradiated mice and controls. Femoral sections from irradiated mice showed that adipocytes increased significantly in irradiated mice; K: Tartrate-resistant acid phosphatase staining of femoral sections from irradiated mice and controls; L: Real-time quantitative polymerase chain reaction (RT-qPCR) analysis of receptor activator of nuclear factor κ B ligand and osteoprotegerin mRNA expression in flushed whole bone marrow; M: Receptor activator of nuclear factor κ B ligand/osteoprotegerin ratio based on RT-qPCR results; N: RT-qPCR analysis of CR6-interacting factor-1 mRNA expression in flushed whole bone marrow; O: Western blot analysis of CR6-interacting factor-1 expression in flushed whole bone marrow. ^a $P < 0.05$, ^b $P < 0.01$, and the bars represent the mean \pm SD. OPG: Osteoprotegerin; RANKL: Receptor activator of nuclear factor κ B ligand; Crif1: CR6-interacting factor-1; BM: Bone marrow; SMI: Structure model index; BV/TV: Bone volume/total volume; Conn.D: Connectivity density; Tb.N: Trabecular number; vBMD: Bone mineral density; Tb.Sp: Trabecular spacing; Tb.Th: Trabecular thickness.

Crif1 is involved in the regulation of RANKL expression after radiation

RANKL provides the critical signal to induce osteoclast differentiation by binding to its receptor RANK (on haematopoietic progenitors, such as monocytes-macrophages)^[6]. To further confirm whether Crif1 plays an important role in osteoclastogenesis after radiation, we knocked out *Crif1* in RAW264.7 cells and BM-MSCs (Figures 3A and 3D), respectively. The deletion of *Crif1* in RAW264.7 cells did

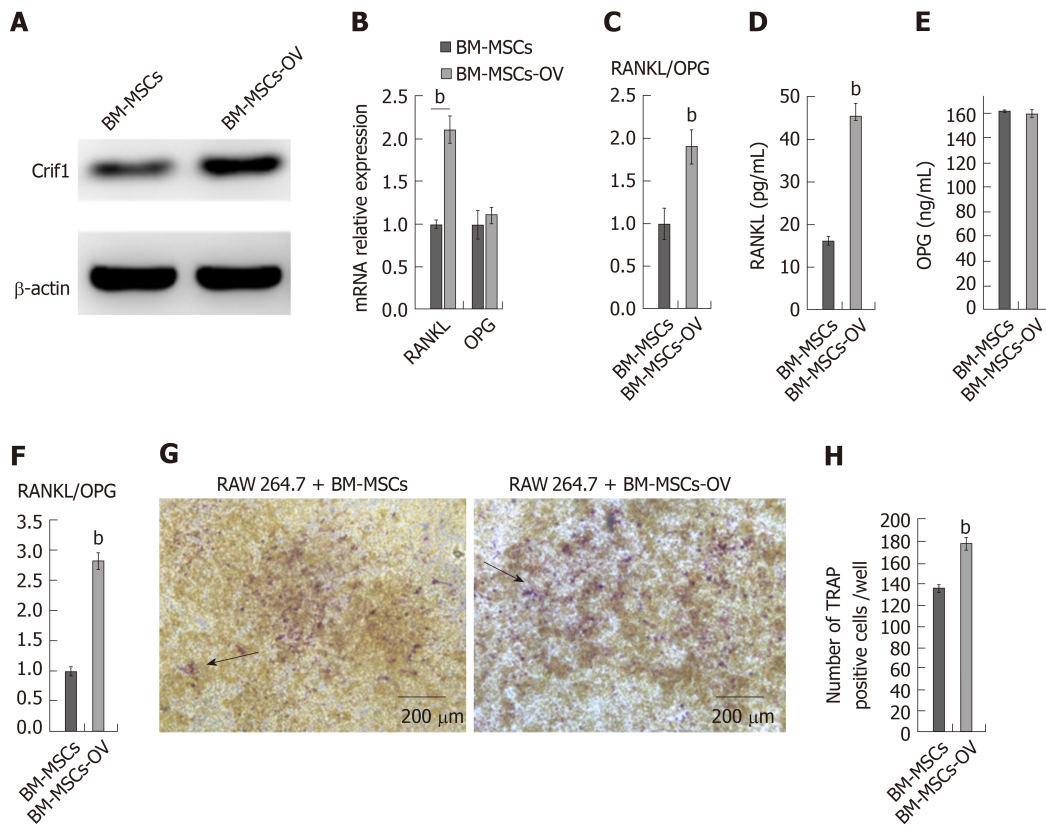


Figure 2 Overexpression of CR6-interacting factor-1 in bone marrow mesenchymal stem/stromal cells increases receptor activator of nuclear factor κ B ligand secretion and osteoclastogenesis. A: Western blot analysis of CR6-interacting factor-1 (Crif1) expression in mouse bone marrow mesenchymal stem/stromal cells (BM-MSCs). Mouse BM-MSCs were transfected with a Crif1 lentiviral overexpression vector; B: Real-time quantitative polymerase chain reaction analysis of receptor activator of nuclear factor κ B ligand (RANKL) and osteoprotegerin (OPG) mRNA expression in BM-MSCs and Crif1-overexpressing BM-MSCs. BM-MSCs and Crif1-overexpressing BM-MSCs were cocultured with RAW264.7, respectively; C: RANKL/OPG ratio based on real-time quantitative polymerase chain reaction results; D: Enzyme linked immunosorbent assay analysis of RANKL protein levels in coculture supernatant medium; E: Enzyme linked immunosorbent assay analysis of OPG protein levels in coculture supernatant medium; F: RANKL/OPG ratio in coculture supernatant medium; G: Tartrate-resistant acid phosphatase staining of RAW264.7 cells after 7 d of coculture; H: Average number of tartrate-resistant acid phosphatase-positive cells/well (arrow) from RAW264.7 cells in coculture. ^a $P < 0.05$, ^b $P < 0.01$, and the bars represent the mean \pm SD. OPG: Osteoprotegerin; RANKL: Receptor activator of nuclear factor κ B ligand; Crif1: CR6-interacting factor-1; BM-MSCs: Bone marrow mesenchymal stem/stromal cells; BM-MSCs-OV: Crif1-overexpressing BM-MSCs.

not affect the RANK expression or osteoclast differentiation (Figure 3A-C). We previously demonstrated that Crif1 expression was upregulated after radiation, and in this study, we found that RANKL expression and the RANKL/OPG ratio were also elevated after radiation (Figure 3E-G and I). Meanwhile, more TRAP-positive cells were found in RAW264.7 cells cocultured with BM-MSCs after radiation (Figure 3J and K). However, knocking out *Crif1* in BM-MSCs could significantly reduce RANKL expression and the RANKL/OPG ratio both before and after radiation (Figure 3E-G and I). OPG expression was not affected by *Crif1* deletion or radiation treatment (Figure 3E and H). Moreover, the number of TRAP-positive cells also decreased in *Crif1* knockout BM-MSCs compared to the control after 7 d of coculture with or without radiation treatment (Figure 3J and K). These results further demonstrated that Crif1 can regulate RANKL expression, especially after radiation.

Crif1 mediates adipogenesis and RANKL secretion in adipocytes

After radiation exposure, the hematopoietic red marrow gradually turns yellow, which is also known as bone marrow fatting. Moreover, excessive numbers of adipocytes are often found in the bone marrow of patients with osteoporosis, and these adipocytes can also secrete RANKL and accelerate osteoclastogenesis^[27]. To determine whether Crif1 affects RANKL expression in adipocytes, BM-MSCs were exposed to a single dose of 9 Gy and then grown in mouse mesenchymal stem cell adipogenic differentiation medium. Consistent with our previous research^[24], more BM-MSCs became strongly predisposed to adipogenesis after radiation treatment. After 21 d of induction, the intensity of oil red O staining was significantly higher in irradiated BM-MSCs, and more adipocytes were found in this group. Important regulators during late adipogenesis, such as PPAR- γ and AP2, both increased after radiation treatment (Figure 4A-C). Here, we also found an obvious increase in

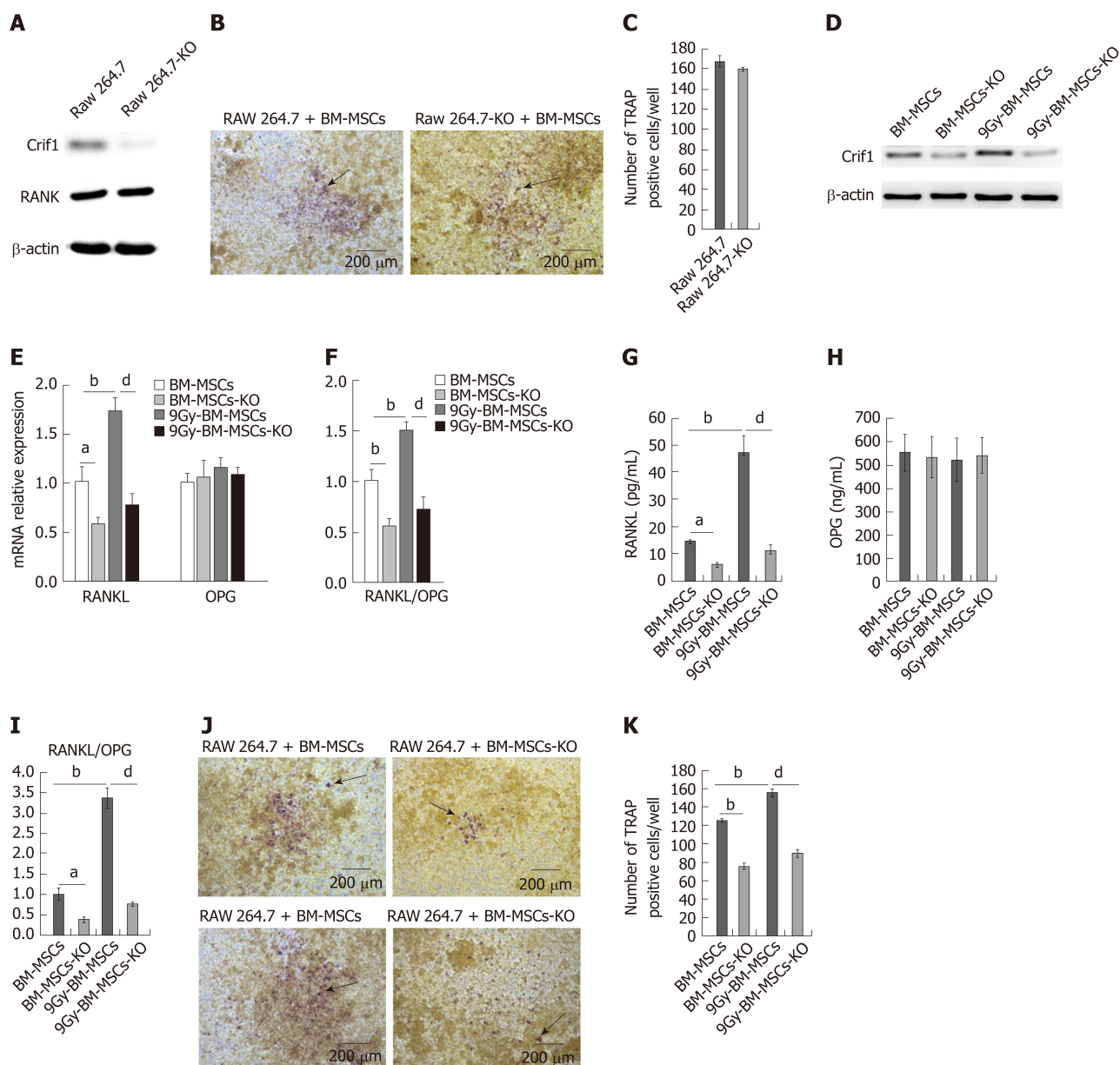


Figure 3 CR6-interacting factor-1 is involved in the regulation of receptor activator of nuclear factor κ B ligand expression after radiation. A: Western blot analysis of CR6-interacting factor-1 (*Crif1*) and receptor activator of nuclear factor κ B expression in RAW264.7 cells. *Crif1* was knocked out in RAW264.7 cells (RAW264.7-KO); B: Tartrate-resistant acid phosphatase (TRAP) staining of RAW264.7-KO and controls after 7 d of coculture with mouse bone marrow mesenchymal stem/stromal cells (BM-MSCs); C: Average number of TRAP-positive cells/well (arrow) from RAW264.7-KO and controls after 7 d of coculture with mouse BM-MSCs; D: Western blot analysis of *Crif1* expression in BM-MSCs. *Crif1* was knocked out in mouse BM-MSCs (BM-MSCs-KO), and BM-MSCs-KO and controls were irradiated with Co-60 at a single dose of 9 Gy; E: Real-time quantitative polymerase chain reaction analysis of receptor activator of nuclear factor κ B ligand (RANKL) and osteoprotegerin (OPG) mRNA expression in BM-MSCs and BM-MSCs-KO. BM-MSCs and BM-MSCs-KO were cocultured with RAW264.7; F: RANKL/OPG ratio based on real-time quantitative polymerase chain reaction results; G: Enzyme linked immunosorbent assay analysis of RANKL protein levels in coculture supernatant medium; H: Enzyme linked immunosorbent assay analysis of OPG protein levels in coculture supernatant medium; I: RANKL/OPG ratio in coculture supernatant medium; J: TRAP staining of RAW264.7 after 7 d of coculture; K: Average number of TRAP-positive cells/well (arrow) from RAW264.7 in coculture. ^a $P < 0.05$ vs control (BM-MSCs), ^b $P < 0.01$ vs control (BM-MSCs), ^c $P < 0.01$ between 9 Gy-BM-MSCs and 9 Gy-BM-MSCs-KO, and the bars represent the mean \pm standard deviation. BM-MSCs: Bone marrow mesenchymal stem/stromal cells; BM-MSCs-KO: *Crif1* was knocked out from mouse BM-MSCs; RAW264.7-KO: *Crif1* was knocked out from RAW264.7 cells; OPG: Osteoprotegerin; RANKL: Receptor activator of nuclear factor κ B ligand.

RANKL expression and RANKL/OPG ratio in irradiated BM-MSCs after adipogenic induction (Figure 4D-F and H). However, knocking out *Crif1* in BM-MSCs reduced adipogenesis (Figure 4A-C), RANKL expression, and RANKL/OPG ratio (Figure 4D-F and H) with or without radiation treatment. OPG expression was not affected by *Crif1* deletion or radiation treatment (Figure 4D and G). These data suggested that *Crif1* mediates adipogenesis and RANKL secretion in adipocytes.

***Crif1* promotes RANKL secretion by modulating the cAMP/PKA signaling pathway**

The regulation of bone remodeling involves many factors, such as parathyroid

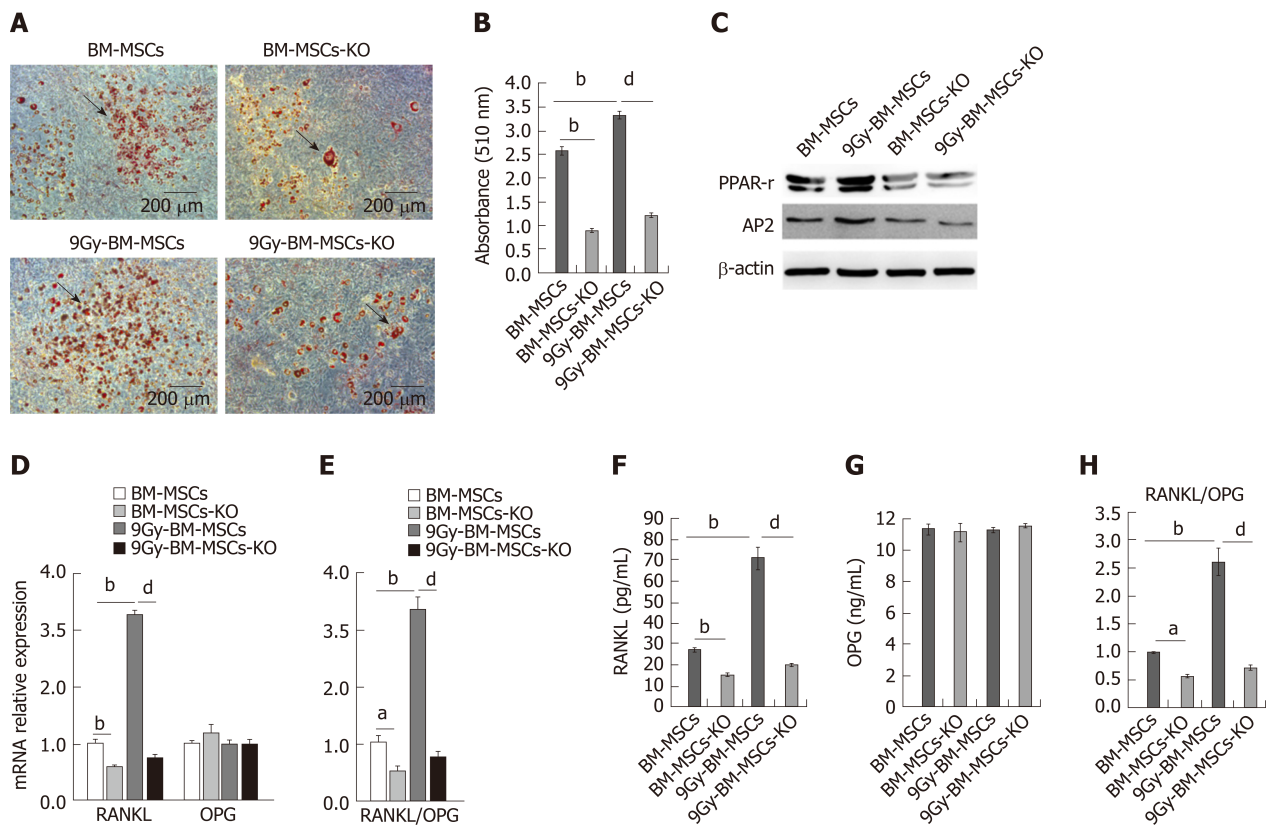
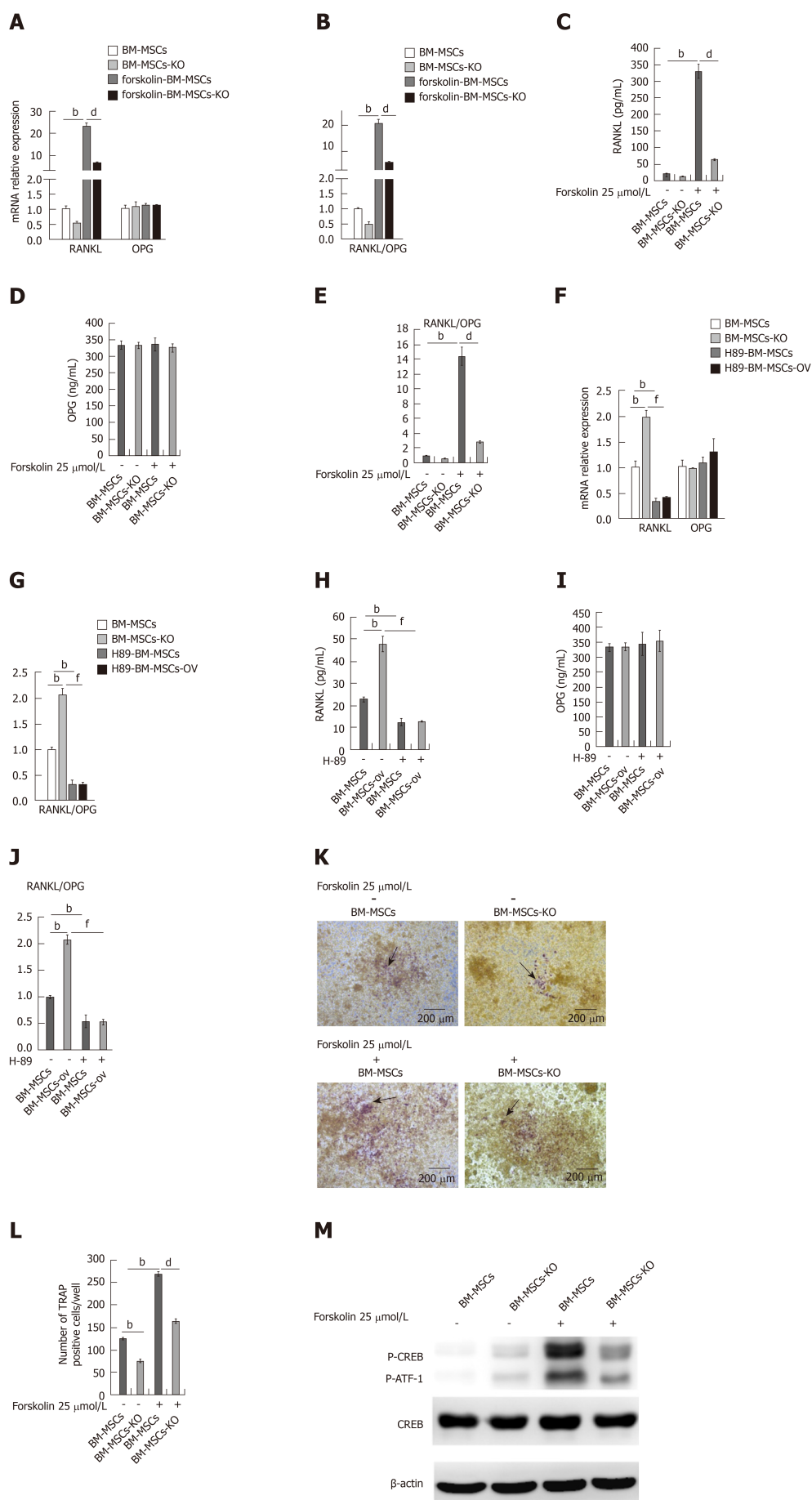


Figure 4 CR6-interacting factor-1 mediates adipogenesis and receptor activator of nuclear factor κ B ligand secretion in adipocytes. A: Oil red O staining analysis of mouse bone marrow mesenchymal stem/stromal cells (BM-MSCs) after 21 d of adipogenic differentiation. *Crif1* was knocked out in mouse BM-MSCs (BM-MSCs-KO), and knockout cells and controls were irradiated with 9 Gy of Co-60, and then treated with mouse mesenchymal stem cell adipogenic differentiation medium (Ad) to induce adipogenesis; B: The dye from oil red O staining was extracted using isopropanol, and the optical density at 510 nm was measured using Benchmark Plus; C: Western blot analysis of adipogenesis-related markers and transcription factors PPAR γ and AP2 in mouse BM-MSCs after 21 d of adipogenic differentiation; D: Real-time quantitative polymerase chain reaction analysis of receptor activator of nuclear factor κ B ligand (RANKL) and osteoprotegerin (OPG) mRNA expression in BM-MSCs and BM-MSCs-KO; E: RANKL/OPG ratio based on real-time quantitative polymerase chain reaction results; F: Enzyme linked immunosorbent assay analysis of RANKL protein levels in supernatant Ad; G: Enzyme linked immunosorbent assay analysis of OPG protein levels in supernatant Ad; H: RANKL/OPG ratio in supernatant Ad. ^a $P < 0.05$ vs control (BM-MSCs), ^b $P < 0.01$ vs control (BM-MSCs); ^d $P < 0.01$ between 9 Gy-BM-MSCs and 9 Gy-BM-MSCs-KO, and the bars represent the mean \pm SD. BM-MSCs: Bone marrow mesenchymal stem/stromal cells; BM-MSCs-KO: *Crif1* knockout mouse BM-MSCs; OPG: Osteoprotegerin; RANKL: Receptor activator of nuclear factor κ B ligand.

hormone (PTH), vitamin D3, bonemarrow-derived growth factors, and cytokines including RANKL. One of the primary mechanisms of bone remodeling is PTH-induced adenosine 3',5'-monophosphate (cAMP), which activates PKA and leads to phosphorylation and activation of CREB resulting in RANKL production^[28]. To verify the mechanism underlying *Crif1*-mediated upregulation of RANKL expression, PKA agonist (forskolin) and inhibitor (H-89) were added to the co-culture system. RANKL expression and the RANKL/OPG ratio were both increased remarkably after treatment with 25 μ mol/L forskolin, however, these effects were significantly weakened in *Crif1* knockout BM-MSCs (Figure 5A-C and E). In addition, RANKL expression and the RANKL/OPG ratio were both decreased when *Crif1*-overexpressing BM-MSCs and controls were treated with 20 μ mol/L H-89 (Figure 5F-H and J). OPG expression was not affected by forskolin or H-89 treatment (Figure 5A, D, F, and H). TRAP-positive cells were increased significantly by adding forskolin, the most TRAP-positive cells were found in the coculture with forskolin-treated BM-MSCs, but this effect was also reduced by *Crif1* deletion (Figure 5K and L). H-89 could inhibit osteoclastogenesis effectively, and the fewest TRAP-positive cells were found in the coculture with H-89-treated *Crif1*-overexpressing BM-MSCs and controls (Figure 5N and O). After the addition of forskolin, CREB phosphorylation was significantly increased in the control BM-MSCs but was dramatically inhibited in *Crif1* knockout BM-MSCs (Figure 5M). We also observed that CREB phosphorylation was suppressed in both *Crif1*-overexpressing BM-MSCs and controls following exposure to H-89 (Figure 5P). These results demonstrated that *Crif1* promotes RANKL expression through the cAMP/PKA signaling pathway.

Crif1 inhibitors effectively suppress RANKL secretion and adipogenesis



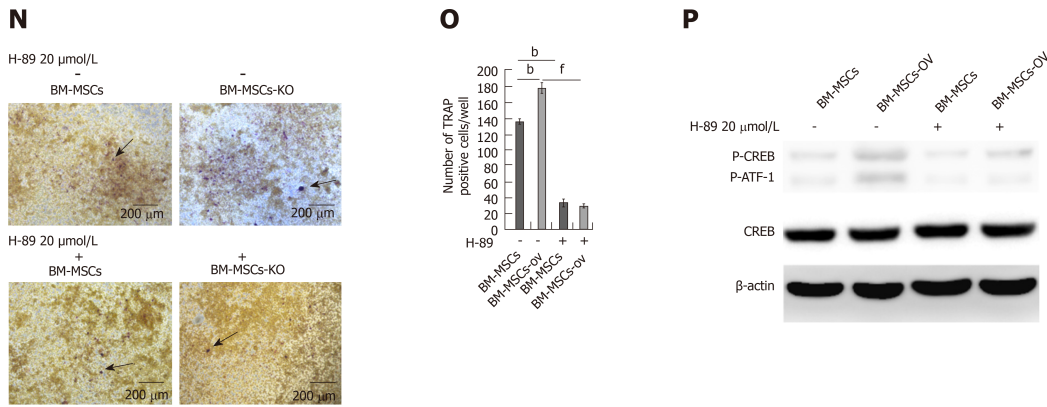


Figure 5 CR6-interacting factor-1 promotes receptor activator of nuclear factor κ B ligand secretion by modulating the cAMP/PKA signaling pathway. A: Real-time quantitative polymerase chain reaction (RT-qPCR) analysis of receptor activator of nuclear factor κ B ligand (RANKL) and osteoprotegerin (OPG) mRNA expression in bone marrow mesenchymal stem/stromal cells (BM-MSCs) and *Crif1* knockout BM-MSCs treated with 25 μ mol/L forskolin in the coculture with RAW264.7; B: RANKL/OPG ratio based on RT-qPCR results; C: Enzyme linked immunosorbent assay (ELISA) analysis of RANKL levels in coculture supernatant medium treated with 25 μ mol/L forskolin; D: ELISA analysis of OPG levels in coculture supernatant medium treated with 25 μ mol/L forskolin; E: RANKL/OPG ratio in coculture supernatant medium treated with 25 μ mol/L forskolin; F: RT-qPCR analysis of RANKL and OPG mRNA expression in BM-MSCs and BM-MSCs-ov treated with 20 μ mol/L H-89 in the coculture with RAW264.7; G: RANKL/OPG ratio based on RT-qPCR results; H: ELISA analysis of RANKL levels in coculture supernatant medium treated with 20 μ mol/L H-89; I: ELISA analysis of OPG levels in coculture supernatant medium treated with 20 μ mol/L H-89; J: RANKL/OPG ratio in coculture supernatant medium treated with 20 μ mol/L H-89; K: Tartrate-resistant acid phosphatase (TRAP) staining of RAW264.7 cells in coculture treated with 25 μ mol/L forskolin; L: Average number of TRAP-positive cells/well (arrow) from RAW264.7 cells in coculture treated with 25 μ mol/L forskolin; M: Western blot analysis of phospho-cyclic adenosine monophosphate response element-binding protein phosphorylation levels in BM-MSCs in coculture treated with 25 μ mol/L forskolin; N: TRAP staining of RAW264.7 in coculture treated with 20 μ mol/L H-89; O: Average number of TRAP-positive cells/well (arrow) from RAW264.7 in coculture treated with 20 μ mol/L H-89; P: Western blot analysis of phospho-cyclic adenosine monophosphate response element-binding protein phosphorylation levels in BM-MSCs in coculture treated with 20 μ mol/L H-89. ^b $P < 0.01$ vs control (BM-MSCs); ^d $P < 0.01$ between between BM-MSCs treated with 25 μ mol/L forskolin and *Crif1* knockout BM-MSCs treated with 25 μ mol/L forskolin; ^f $P < 0.01$ between *Crif1*-overexpressing BM-MSCs and *Crif1*-overexpressing BM-MSCs treated with 20 μ mol/L H-89, and the bars represent the mean \pm SD. BM-MSCs: Bone marrow mesenchymal stem/stromal cells; BM-MSCs-KO: *Crif1* knockout BM-MSCs; OPG: Osteoprotegerin; RANKL: Receptor activator of nuclear factor κ B ligand; CREB: Cyclic adenosine monophosphate response element-binding protein.

Because of the central role of RANKL in osteoclastogenesis, it is the basis for a new therapy to inhibit bone loss. We used ClusPro and InterProSurf to investigate the interaction interface in *Crif1*-PRKACA complex, and the results showed that Thr¹⁹⁷, Gly²⁰⁰, Thr²⁰¹, Glu²⁰³, and Phe¹²⁹ of PRKACA interact with Ile¹³², Met¹²⁸, Ile¹²¹, His¹²⁰, and Arg¹¹⁷ in the long α -helical region of *Crif1*, forming the binding interface (Figure 6A). Virtual screening using 462608 compounds from the Life Chemicals database around His¹²⁰ of *Crif1* was carried out using the program Autodock_vina. A set of 13 compounds was selected for experimental screening based on binding energy < -12.0 kcal/mol (Supplementary Table 1). The binding pattern in the best-scored ligand-protein complexes potentially contained multiple interactions dominated by hydrophobic amino acids (Figure 6B-F). Initially, a tetrazolium salt (WST-8) assay was carried out to study the potentially toxic effects of these compounds on different cell lines, including human BM-MSCs, Vero cells, and mouse BM-MSCs (Supplementary Figures 1-3). The compounds F0382-0033, F3408-0076, F1430-0134, F3408-0031, and F1430-0130 showed low toxicity to hBM-MSCs at a concentration of 25 μ mol/L (Figures 6G-6K). To determine whether these compounds could affect RANKL expression, H-BM-MSCs were pretreated with these compounds followed by treatment with forskolin. ELISA analysis of supernatant medium revealed that RANKL expression was dramatically decreased by treatment with five *Crif1* inhibitors (Figure 7A). OPG expression could be significantly increased by F1430-0134, but there were no significant differences between the other four compounds and the control (Figure 7B). Moreover, RANKL/OPG ratios were also decreased by these five compounds compared with the control (Figure 7C). *Crif1* is involved in adipogenesis^[24], and adipocytes are also the source of RANKL in the bone marrow^[27]. In order to study the inhibitory effects of these five compounds on adipogenic differentiation of BM-MSCs, H-BM-MSCs were pretreated with five different compounds (25 μ mol/L) followed by adipogenic induction. Oil red O staining indicated that adipogenic differentiation of H-BM-MSCs was remarkably suppressed by the addition of these five compounds (Figure 7D and E). To further understand the mechanism, CREB phosphorylation was detected. Western blot analysis showed that CREB phosphorylation activated by forskolin was significantly inhibited by pretreatment with the five compounds (Figure 7F). These results showed that *Crif1* inhibitors could effectively suppress RANKL secretion and adipogenesis by inhibiting

CREB phosphorylation.

DISCUSSION

Radiation exposure (due to radiotherapy, accidental causes, or terrorism) causes irreparable damage to tissues and organs, and both the bone marrow and bone architecture are devastated following radiation exposure. Irradiation causes rapid depletion of bone marrow, total extracted bone marrow cells in the irradiated mice, including the hematopoietic cell niches, collapsed by $65\% \pm 11\%$ after 2 d, remaining at those levels through 10 d^[29]. In contrast, the number of CD90⁺, CD29⁺, CD45⁺, and CD11b⁺ BM-MSCs increased relatively^[24]. Irradiation also changes the bone marrow microenvironment, and adipocytes are significantly increased after radiation in the medullary cavity, which can negatively regulate the hematopoietic microenvironment, inhibit hematopoiesis, and accelerate osteoclastogenesis^[30,31]. Irradiation suppresses bone formation and elevates bone resorption, disturbing the balance between them and leading to a dramatic decline in trabecular bone^[32]. There is a near-immediate reduction in the number of osteoblasts, but an increased number and activity of osteoclasts post-radiation therapy^[33]. In this study, we treated mice with a single dose of 5 Gy to generate a model of radiation-induced osteoporosis. RANKL expression and RANKL/OPG ratios actually increased in the surviving bone marrow cells after radiation, which was consistent with a previous study^[14]. Meanwhile, expression of Crif1 and bone resorption also increased, indicating a relationship between RANKL and Crif1 in osteoporosis.

BM-MSCs, which are a major and important component of the bone marrow microenvironment, are the progenitors of both bone marrow osteoblasts and adipocytes. The balance between osteogenic and adipogenic differentiation of BM-MSCs plays a pivotal role in supporting hematopoiesis and maintaining bone homeostasis^[34,35]. Crosstalk between macrophages and BM-MSCs within the bone marrow is also important for bone homeostasis. Different macrophage phenotypes exert different biological effects on the differentiation of BM-MSCs. Moreover, the modulatory effects of BM-MSCs on osteoclast progenitors, such as the monocyte-macrophage lineage, could be mediated by secretion of soluble factors^[36,37]. Compared to other cells in bone marrow, BM-MSCs are more resistant to radiation, so the remaining BM-MSCs that escape radiation killing is crucial for the bone marrow microenvironment^[38]. Following radiation exposure, BM-MSCs appear to preferentially differentiate into adipocytes instead of osteoblasts. This can ultimately hinder the proper bone formation and lead to disorders associated with bone loss (*e.g.*, osteoporosis) or increased adipocyte content, ultimately leading to hematopoietic progenitor cell depletion^[12]. Excessive numbers of adipocytes are often found in the bone marrow of patients with osteoporosis. It is indicated that the shift of the cell differentiation of BM-MSCs to adipocytes rather than osteoblasts partly contributes to osteoporosis^[39]. A recent study revealed that bone marrow adipocytes can also secrete RANKL and accelerate osteoclastogenesis^[27]. We previously reported that Crif1 can promote the adipogenesis of BM-MSCs after radiation. Here, we found that Crif1 could also promote RANKL secretion by BM-MSCs after radiation, and the deletion of *Crif1* in BM-MSCs and Crif1 inhibitors can reduce both adipogenesis and RANKL expression.

RANKL functions as an osteoclast-activating factor, and its binding to RANK induces the activation of transcription factors such as c-fos, NFAT, and nuclear factor kappa B in preosteoclasts and initiates several downstream signaling pathways, especially the NF- κ B pathway^[40]. As RANKL is the only known ligand for RANK, and RANK and RANKL are crucial in bone metabolism, it is important to understand how the expression levels of RANKL are regulated under normal and disease conditions. RANKL expression can be upregulated by many agents, such as PTH and forskolin. Forskolin can stimulate RANKL expression through the cAMP/PKA signaling pathway^[41]. It has been proved that cytokines and hormones which promote osteoclast formation act first on osteoblast lineage cells to promote the production of RANKL^[42]. In this study, following forskolin exposure, RANKL expression increased significantly in BM-MSCs. However, the deletion of Crif1 from BM-MSCs impairs the promotion of RANKL expression by forskolin. Moreover, overexpression of Crif1 in BM-MSCs does not increase RANKL expression upon exposure to a PKA inhibitor. Here, we further demonstrated that Crif1 could also promote RANKL expression through the cAMP/PKA signaling pathway.

Drugs for the treatment of osteoporosis could be divided into anabolic and antiresorptive categories. Bisphosphonates (including alendronate and ibandronate, target osteoclast), estrogen, selective estrogen receptor modulators, and denosumab

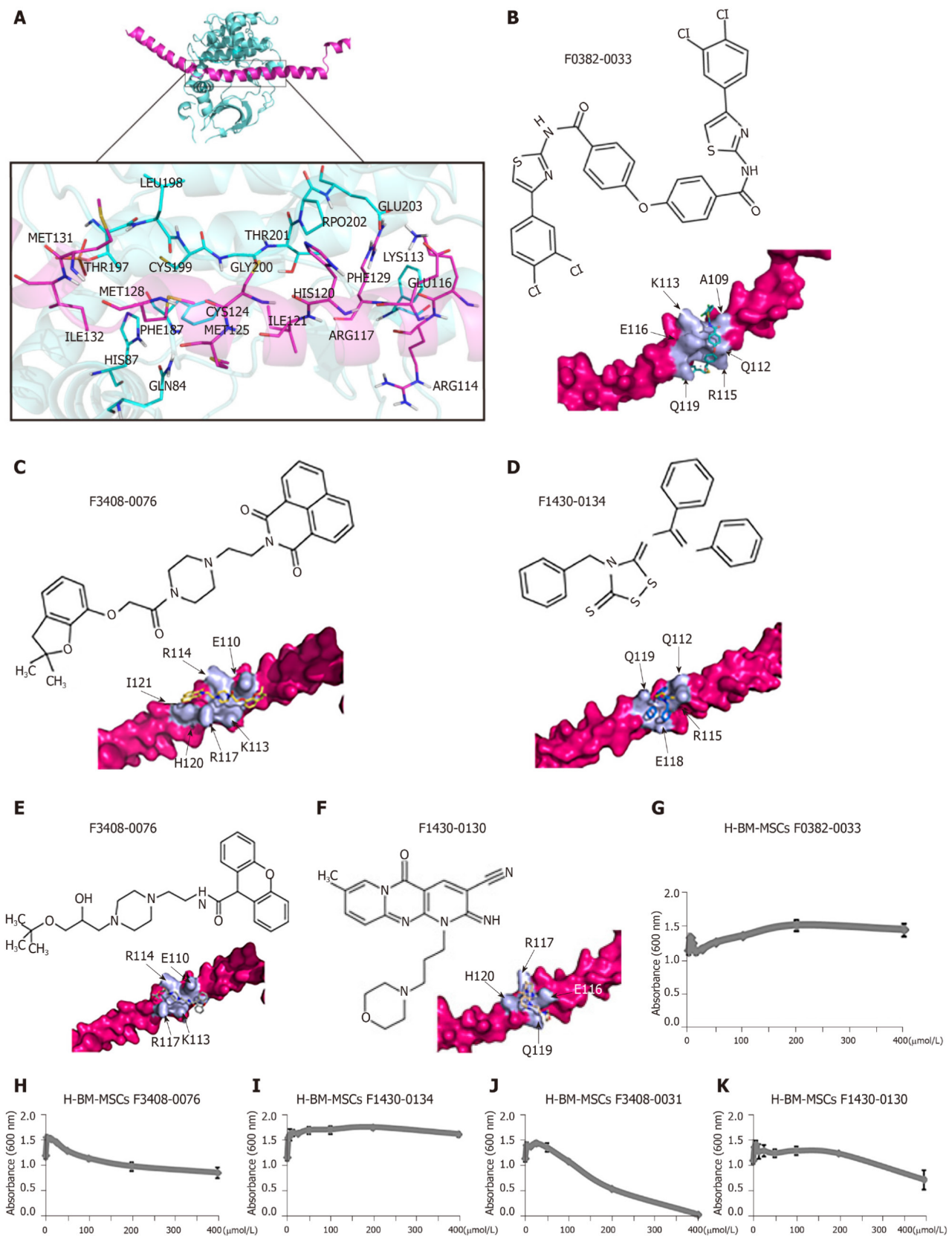


Figure 6 CR6-interacting factor-1-protein kinase cyclic adenosine monophosphate-activated catalytic subunit alpha interaction model and the inhibition potential of the lowest toxic effect of compounds. **A:** CR6-interacting factor-1 (Crif1)-protein kinase cyclic adenosine monophosphate-activated catalytic subunit alpha (PRKACA) interaction model showing Crif1 (colored in rose red) and PRKACA (colored in cyan). Interface amino acids are shown as sticks and colored in rose red (for Crif1) and cyan (for PRKACA) and indicated as a zoomed-in view in the inset figure; **B-F:** Chemical structure of each inhibitor molecule and their docked pose on Crif1 (colored in rose red, surface view). Docked molecule (stick) and the amino acids involved in the hydrophobic interactions (light purple) are shown. F0382-0033 (**B**), F3408-0076 (**C**), F1430-0134 (**D**), F3408-0031 (**E**), and F1430-0130 (**F**); **G-K:** A tetrazolium salt (WST-8) assay was carried out to study the toxic effect of compounds on the H-BM-MSCs. F0382-0033 (**G**), F3408-0076 (**H**), F1430-0134 (**I**), F3408-0031 (**J**), and F1430-0130 (**K**). The bars represent the mean \pm standard deviation. H-BM-MSCs: Human bone marrow mesenchymal stem/stromal cells.

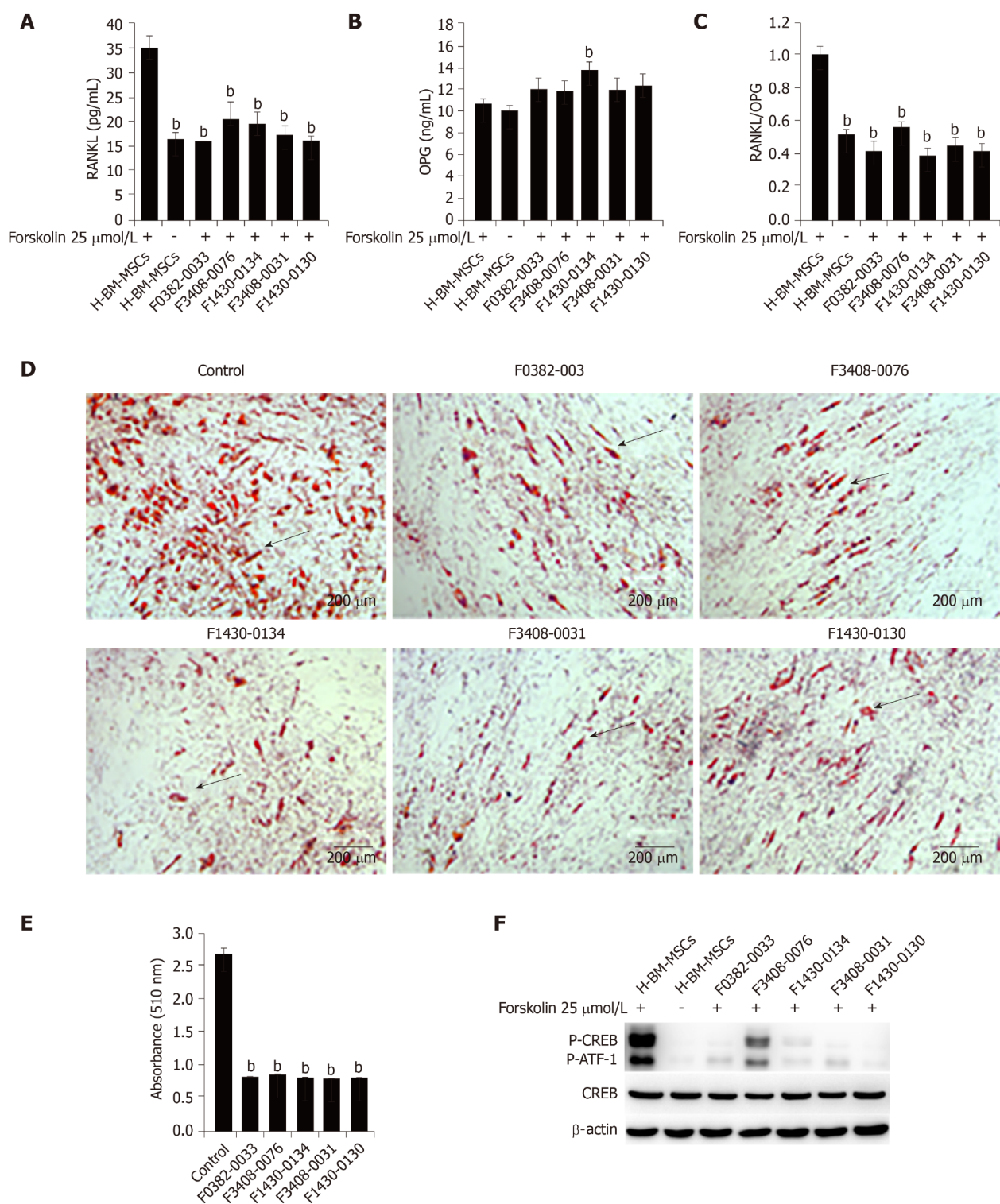


Figure 7 CR6-interacting factor-1 inhibitors effectively suppress receptor activator of nuclear factor κ B ligand secretion and adipogenesis. A: Enzyme linked immunosorbent assay (ELISA) analysis of receptor activator of nuclear factor κ B ligand protein levels in the supernatant medium. Human bone marrow mesenchymal stem/stromal cells (H-BM-MSCs) were pretreated with five different compounds (25 $\mu\text{mol/L}$) followed by treatment with forskolin (25 $\mu\text{mol/L}$), and supernatant medium was collected for ELISA after 3 d; B: ELISA analysis of osteoprotegerin protein levels in supernatant medium; C: Receptor activator of nuclear factor κ B ligand/osteoprotegerin ratio in supernatant medium; D: Oil red O staining analysis of H-BM-MSCs after 21 d of adipogenic differentiation. H-BM-MSCs were pretreated with five different compounds (25 $\mu\text{mol/L}$) followed by adipogenic induction; E: The dye from oil red O staining was extracted using isopropanol, and the optical density at 510 nm was measured using Benchmark Plus; F: Western blot analysis of cyclic adenosine monophosphate response element-binding protein phosphorylation levels. H-BM-MSCs were pretreated with five different compounds (25 $\mu\text{mol/L}$) followed by treatment with forskolin (25 $\mu\text{mol/L}$) and total protein lysates were extracted for cyclic adenosine monophosphate response element-binding protein phosphorylation detection after 1 h. ^a $P < 0.05$, ^b $P < 0.01$, and the bars represent the mean \pm SD. OPG: Osteoprotegerin; RANKL: Receptor activator of nuclear factor κ B ligand; CREB: Cyclic adenosine monophosphate response element-binding protein; H-BM-MSCs: Human bone marrow mesenchymal stem/stromal cells.

(an antibody to RANKL) are antiresorptive drugs, whereas PTH and its analogs are

anabolic agents^[43-45]. However, long-term trials showed that these drugs had no effects on the prevention of hip fractures. Moreover, the adverse effects of these anti-osteoporotic drugs should also be considered, such as hypocalcemia, arthralgia, nausea, and especially the development of breast cancer and risks of cardiovascular events and thromboembolism associated with treatment with estrogen and selective estrogen receptor modulators^[46]. Mesenchymal stem/stromal cells (MSCs) are one of the favorite sources of cell-based therapy. MSCs-based preclinical studies in animal models suggest a great clinical application potential of both BM-MSCs and adipose tissue-derived MSCs for osteoporosis treatment. However, the bone marrow homing efficiency, the long-term survival, and the uncertainty of MSCs' fate after cell transplantation are the main concerns on the clinical application of MSCs for osteoporosis^[47]. Therefore, it is necessary to look for alternative treatments with high efficiency but a few side effects. Because of the importance of RANKL in osteoclast differentiation, RANKL-secreting cells, which play a central role in osteoclastogenesis, are the targets of most antiresorptive agents^[48,49]. BM-MSCs could be the target cells, and improving bone marrow microenvironment based on the remaining BM-MSCs in the bone marrow of patients and accelerating osteogenesis based on their fate decision to osteoblast or adipocyte could be a potential treatment for patients with radiation-induced bone injury. Our studies demonstrated that Crif1 could promote RANKL expression and adipogenic differentiation of BM-MSCs after radiation, and this may provide a potential molecular target for osteoporosis treatment. Osteogenesis and adipogenesis in the bone marrow are inversely correlated, so reduced adipogenesis results in an increase in the osteoblast pool^[50,51]. Future drug screening should target not only the regulation of the balance between bone formation and bone resorption but also the balance between osteogenic and adipogenic differentiation.

In conclusion, we have demonstrated that Crif1 plays a crucial role in osteoclastogenesis by inducing RANKL expression through the cAMP/PKA signaling pathway in mice. Moreover, through screening, we have identified five Crif1 inhibitors targeting Crif1-PRKACA interaction interface that could dramatically reduce RANKL secretion and adipogenesis. But the specificity of these five compounds and their effects on bone metabolism, such as increasing bone formation and decreasing bone resorption and adipogenesis, still need further *in vitro* and *in vivo* research, and to be validated in clinical trials. This study nevertheless enriches current knowledge of the pathogenesis of radiation-induced osteoporosis and provides insights into potential therapeutic strategies for radiation-induced bone injury.

ARTICLE HIGHLIGHTS

Research background

Radiation induces rapid bone loss and enhances bone resorption and adipogenesis, leading to an increased risk of bone fracture. Receptor activator of nuclear factor κ B ligand (RANKL) provides the crucial signal to induce osteoclast differentiation and plays an important role in bone resorption. However, the mechanisms of radiation-induced osteoporosis are not fully understood.

Research motivation

Current treatment of osteoporosis is based mainly on inhibiting bone resorption or stimulating bone generation to increase bone mass, however, the side-effects of some drugs affect long-term administration and adherence. There is still a lack of effective preventive or therapeutic method for radiation-induced bone injury. Therefore, it is necessary to look for alternative treatments with high efficiency but few side effects.

Research objectives

In this study, we aimed to investigate the role of CR6-interacting factor-1 (Crif1) in osteoclastogenesis after radiation and its possible mechanism.

Research methods

C57BL/6 mice were exposed to Co-60 gamma rays and received 5 Gy of whole-body sublethal irradiation at a rate of 0.69 Gy/min. For *in vitro* study, mouse bone marrow mesenchymal stem/stromal cells (BM-MSCs) were irradiated with Co-60 at a single dose of 9 Gy. For osteoclast induction, monocyte-macrophage RAW264.7 cells were cocultured with mouse BM-MSCs for 7 d. ClusPro and InterProSurf were used to investigate the interaction interface in Crif1 and protein kinase cyclic adenosine monophosphate (cAMP)-activated catalytic subunit alpha (PRKACA) complex. Virtual screening using 462608 compounds from the Life Chemicals database around His120 of Crif1 was carried out using the program Autodock_vina. A tetrazolium salt (WST-8) assay was carried out to study the toxicity of compounds to different cells, including human BM-MSCs, mouse BM-MSCs, and Vero cells.

Research results

Crif1 expression increased in bone marrow cells after radiation in mice. Overexpression of Crif1 in mouse BM-MSCs and radiation exposure could increase RANKL secretion and promote osteoclastogenesis *in vitro*. Deletion of Crif1 in BM-MSCs could reduce both adipogenesis and RANKL expression, resulting in the inhibition of osteoclastogenesis. The deletion of Crif1 in RAW264.7 cells did not affect the RANK expression or osteoclast differentiation. Following treatment with protein kinase A (PKA) agonist (forskolin) and inhibitor (H-89) in mouse BM-MSCs, Crif1 induced RANKL secretion *via* the cAMP/PKA pathway. Moreover, we identified the Crif1-PRKACA interaction interface by *in silico* studies and shortlisted interface inhibitors through virtual screening on Crif1. Five compounds dramatically suppressed RANKL secretion and adipogenesis by inhibiting the cAMP/PKA pathway.

Research conclusions

Crif1 promotes RANKL expression *via* the cAMP/PKA pathway, which induces osteoclastogenesis by binding to RANK on monocytes-macrophages in the mouse model. These results suggest a role for Crif1 in modulating osteoclastogenesis and provide insights into potential therapeutic strategies targeting the balance between osteogenesis and adipogenesis for radiation-induced bone injury.

Research perspectives

Because of the contribution of adipocytes to osteoporosis, future drug screening should target not only the regulation of the balance between bone formation and bone resorption but also the balance between osteogenic and adipogenic differentiation. Here, through screening, we identified five Crif1 inhibitors targeting Crif1-PRKACA interaction interface that could dramatically reduce RANKL secretion and adipogenesis. Our study provides insights into potential therapeutic strategies for radiation-induced bone injury.

REFERENCES

- Green DE, Rubin CT. Consequences of irradiation on bone and marrow phenotypes, and its relation to disruption of hematopoietic precursors. *Bone* 2014; **63**: 87-94 [PMID: 24607941 DOI: 10.1016/j.bone.2014.02.018]
- Jia D, Gaddy D, Suva LJ, Corry PM. Rapid loss of bone mass and strength in mice after abdominal irradiation. *Radiat Res* 2011; **176**: 624-635 [PMID: 21859327 DOI: 10.1667/rr2505.1]
- Baxter NN, Habermann EB, Tepper JE, Durham SB, Virnig BA. Risk of pelvic fractures in older women following pelvic irradiation. *JAMA* 2005; **294**: 2587-2593 [PMID: 16304072 DOI: 10.1001/jama.294.20.2587]
- Rachner TD, Khosla S, Hofbauer LC. Osteoporosis: now and the future. *Lancet* 2011; **377**: 1276-1287 [PMID: 21450337 DOI: 10.1016/S0140-6736(10)62349-5]
- Khosla S, Hofbauer LC. Osteoporosis treatment: recent developments and ongoing challenges. *Lancet Diabetes Endocrinol* 2017; **5**: 898-907 [PMID: 28689769 DOI: 10.1016/S2213-8587(17)30188-2]
- Teitelbaum SL. Bone resorption by osteoclasts. *Science* 2000; **289**: 1504-1508 [PMID: 10968780 DOI: 10.1126/science.289.5484.1504]
- Boyle WJ, Simonet WS, Lacey DL. Osteoclast differentiation and activation. *Nature* 2003; **423**: 337-342 [PMID: 12748652 DOI: 10.1038/nature01658]
- Boyce BF, Xing L. Biology of RANK, RANKL, and osteoprotegerin. *Arthritis Res Ther* 2007; **9** Suppl 1: S1 [PMID: 17634140 DOI: 10.1186/ar2165]
- Wada T, Nakashima T, Hiroshi N, Penninger JM. RANKL-RANK signaling in osteoclastogenesis and bone disease. *Trends Mol Med* 2006; **12**: 17-25 [PMID: 16356770 DOI: 10.1016/j.molmed.2005.11.007]
- Nakashima T, Hayashi M, Fukunaga T, Kurata K, Oh-Hora M, Feng JQ, Bonewald LF, Kodama T, Wutz A, Wagner EF, Penninger JM, Takayanagi H. Evidence for osteocyte regulation of bone homeostasis through RANKL expression. *Nat Med* 2011; **17**: 1231-1234 [PMID: 21909105 DOI: 10.1038/nm.2452]
- Boyce BF, Xing L. Functions of RANKL/RANK/OPG in bone modeling and remodeling. *Arch Biochem Biophys* 2008; **473**: 139-146 [PMID: 18395508 DOI: 10.1016/j.abb.2008.03.018]
- Nuttall ME, Gimble JM. Controlling the balance between osteoblastogenesis and adipogenesis and the consequent therapeutic implications. *Curr Opin Pharmacol* 2004; **4**: 290-294 [PMID: 15140422 DOI: 10.1016/j.coph.2004.03.002]
- Islam MS, Stemig ME, Takahashi Y, Hui SK. Radiation response of mesenchymal stem cells derived from bone marrow and human pluripotent stem cells. *J Radiat Res* 2015; **56**: 269-277 [PMID: 25425005 DOI: 10.1093/jrr/rru098]
- Alwood JS, Shahnazari M, Chicana B, Schreurs AS, Kumar A, Bartolini A, Shirazi-Fard Y, Globus RK. Ionizing Radiation Stimulates Expression of Pro-Osteoclastogenic Genes in Marrow and Skeletal Tissue. *J Interferon Cytokine Res* 2015; **35**: 480-487 [PMID: 25734366 DOI: 10.1089/jir.2014.0152]
- Chung HK, Yi YW, Jung NC, Kim D, Suh JM, Kim H, Park KC, Song JH, Kim DW, Hwang ES, Yoon SH, Bae YS, Kim JM, Bae I, Shong M. CR6-interacting factor 1 interacts with Gadd45 family proteins and modulates the cell cycle. *J Biol Chem* 2003; **278**: 28079-28088 [PMID: 12716909 DOI: 10.1074/jbc.M212835200]
- Ran Q, Hao P, Xiao Y, Xiang L, Ye X, Deng X, Zhao J, Li Z. CRIF1 interacting with CDK2 regulates bone marrow microenvironment-induced G0/G1 arrest of leukemia cells. *PLoS One* 2014; **9**: e85328 [PMID: 24520316 DOI: 10.1371/journal.pone.0085328]
- Park KC, Song KH, Chung HK, Kim H, Kim DW, Song JH, Hwang ES, Jung HS, Park SH, Bae I, Lee IK, Choi HS, Shong M. CR6-interacting factor 1 interacts with orphan nuclear receptor Nur77 and inhibits its transactivation. *Mol Endocrinol* 2005; **19**: 12-24 [PMID: 15459248 DOI: 10.1210/me.2004-0107]
- Kang HJ, Hong YB, Kim HJ, Bae I. CR6-interacting factor 1 (CRIF1) regulates NF-E2-related factor 2 (NRF2) protein stability by proteasome-mediated degradation. *J Biol Chem* 2010; **285**: 21258-21268 [PMID: 20427290 DOI: 10.1074/jbc.M109.084590]
- Chen L, Ran Q, Xiang Y, Xiang L, Chen L, Li F, Wu J, Wu C, Li Z. Co-Activation of PKC- δ by CRIF1 Modulates Oxidative Stress in Bone Marrow Multipotent Mesenchymal Stromal Cells after Irradiation by

- Phosphorylating NRF2 Ser40. *Theranostics* 2017; **7**: 2634-2648 [PMID: [28819452](#) DOI: [10.7150/thno.17853](#)]
- 20 **Ran Q**, Xiang Y, Stephen P, Wu C, Li T, Lin SX, Li Z. CRIF1-CDK2 Interface Inhibitors: An Unprecedented Strategy for Modulation of Cell Radiosensitivity. *J Am Chem Soc* 2019; **141**: 1420-1424 [PMID: [30653304](#) DOI: [10.1021/jacs.8b10207](#)]
- 21 **Ran Q**, Jin F, Xiang Y, Xiang L, Wang Q, Li F, Chen L, Zhang Y, Wu C, Zhou L, Xiao Y, Chen L, Wu J, Zhong JF, Li SC, Li Z. CRIF1 as a potential target to improve the radiosensitivity of osteosarcoma. *Proc Natl Acad Sci USA* 2019; **116**: 20511-20516 [PMID: [31548420](#) DOI: [10.1073/pnas.1906578116](#)]
- 22 **Greber BJ**, Bieri P, Leibundgut M, Leitner A, Aebersold R, Boehringer D, Ban N. Ribosome. The complete structure of the 55S mammalian mitochondrial ribosome. *Science* 2015; **348**: 303-308 [PMID: [25837512](#) DOI: [10.1126/science.aaa3872](#)]
- 23 **Jung SB**, Choi MJ, Ryu D, Yi HS, Lee SE, Chang JY, Chung HK, Kim YK, Kang SG, Lee JH, Kim KS, Kim HJ, Kim CS, Lee CH, Williams RW, Kim H, Lee HK, Auwerx J, Shong M. Reduced oxidative capacity in macrophages results in systemic insulin resistance. *Nat Commun* 2018; **9**: 1551 [PMID: [29674655](#) DOI: [10.1038/s41467-018-03998-z](#)]
- 24 **Zhang X**, Xiang L, Ran Q, Liu Y, Xiang Y, Xiao Y, Chen L, Li F, Zhong JF, Li Z. Crif1 Promotes Adipogenic Differentiation of Bone Marrow Mesenchymal Stem Cells After Irradiation by Modulating the PKA/CREB Signaling Pathway. *Stem Cells* 2015; **33**: 1915-1926 [PMID: [25847389](#) DOI: [10.1002/stem.2019](#)]
- 25 **Chen MF**, Lin CT, Chen WC, Yang CT, Chen CC, Liao SK, Liu JM, Lu CH, Lee KD. The sensitivity of human mesenchymal stem cells to ionizing radiation. *Int J Radiat Oncol Biol Phys* 2006; **66**: 244-253 [PMID: [16839703](#) DOI: [10.1016/j.ijrobp.2006.03.062](#)]
- 26 **Jiang Y**, Jahagirdar BN, Reinhardt RL, Schwartz RE, Keene CD, Ortiz-Gonzalez XR, Reyes M, Lenvik T, Lund T, Blackstad M, Du J, Aldrich S, Lisberg A, Low WC, Largaespada DA, Verfaillie CM. Pluripotency of mesenchymal stem cells derived from adult marrow. *Nature* 2002; **418**: 41-49 [PMID: [12077603](#) DOI: [10.1038/nature00870](#)]
- 27 **Fan Y**, Hanai JI, Le PT, Bi R, Maridas D, DeMambro V, Figueroa CA, Kir S, Zhou X, Mannstadt M, Baron R, Bronson RT, Horowitz MC, Wu JY, Bilezikian JP, Dempster DW, Rosen CJ, Lanske B. Parathyroid Hormone Directs Bone Marrow Mesenchymal Cell Fate. *Cell Metab* 2017; **25**: 661-672 [PMID: [28162969](#) DOI: [10.1016/j.cmet.2017.01.001](#)]
- 28 **Kondo H**, Guo J, Bringham FR. Cyclic adenosine monophosphate/protein kinase A mediates parathyroid hormone/parathyroid hormone-related protein receptor regulation of osteoclastogenesis and expression of RANKL and osteoprotegerin mRNAs by marrow stromal cells. *J Bone Miner Res* 2002; **17**: 1667-1679 [PMID: [12211438](#) DOI: [10.1359/jbmr.2002.17.9.1667](#)]
- 29 **Green DE**, Adler BJ, Chan ME, Rubin CT. Devastation of adult stem cell pools by irradiation precedes collapse of trabecular bone quality and quantity. *J Bone Miner Res* 2012; **27**: 749-759 [PMID: [22190044](#) DOI: [10.1002/jbmr.1505](#)]
- 30 **Cao X**, Wu X, Frassica D, Yu B, Pang L, Xian L, Wan M, Lei W, Armour M, Tryggstad E, Wong J, Wen CY, Lu WW, Frassica FJ. Irradiation induces bone injury by damaging bone marrow microenvironment for stem cells. *Proc Natl Acad Sci USA* 2011; **108**: 1609-1614 [PMID: [21220327](#) DOI: [10.1073/pnas.1015350108](#)]
- 31 **Naveiras O**, Nardi V, Wenzel PL, Hauschka PV, Fahey F, Daley GQ. Bone-marrow adipocytes as negative regulators of the haematopoietic microenvironment. *Nature* 2009; **460**: 259-263 [PMID: [19516257](#) DOI: [10.1038/nature08099](#)]
- 32 **D'Oronzo S**, Stucci S, Tucci M, Silvestris F. Cancer treatment-induced bone loss (CTIBL): pathogenesis and clinical implications. *Cancer Treat Rev* 2015; **41**: 798-808 [PMID: [26410578](#) DOI: [10.1016/j.ctrv.2015.09.003](#)]
- 33 **Pacheco R**, Stock H. Effects of radiation on bone. *Curr Osteoporos Rep* 2013; **11**: 299-304 [PMID: [24057133](#) DOI: [10.1007/s11914-013-0174-z](#)]
- 34 **Mori K**, Suzuki K, Hozumi A, Goto H, Tomita M, Koseki H, Yamashita S, Osaki M. Potentiation of osteoclastogenesis by adipogenic conversion of bone marrow-derived mesenchymal stem cells. *Biomed Res* 2014; **35**: 153-159 [PMID: [24759183](#) DOI: [10.2220/biomedres.35.153](#)]
- 35 **Yue R**, Zhou BO, Shimada IS, Zhao Z, Morrison SJ. Leptin Receptor Promotes Adipogenesis and Reduces Osteogenesis by Regulating Mesenchymal Stromal Cells in Adult Bone Marrow. *Cell Stem Cell* 2016; **18**: 782-796 [PMID: [27053299](#) DOI: [10.1016/j.stem.2016.02.015](#)]
- 36 **He XT**, Li X, Yin Y, Wu RX, Xu XY, Chen FM. The effects of conditioned media generated by polarized macrophages on the cellular behaviours of bone marrow mesenchymal stem cells. *J Cell Mol Med* 2018; **22**: 1302-1315 [PMID: [29106032](#) DOI: [10.1111/jcmm.13431](#)]
- 37 **Sharaf-Eldin WE**, Abu-Shahba N, Mahmoud M, El-Badri N. The Modulatory Effects of Mesenchymal Stem Cells on Osteoclastogenesis. *Stem Cells Int* 2016; **2016**: 1908365 [PMID: [26823668](#) DOI: [10.1155/2016/1908365](#)]
- 38 **Fekete N**, Erle A, Amann EM, Fürst D, Rojewski MT, Langonné A, Sensebé L, Schrezenmeier H, Schmidtke-Schrezenmeier G. Effect of high-dose irradiation on human bone-marrow-derived mesenchymal stromal cells. *Tissue Eng Part C Methods* 2015; **21**: 112-122 [PMID: [24918644](#) DOI: [10.1089/ten.TEC.2013.0766](#)]
- 39 **Liao L**, Yang X, Su X, Hu C, Zhu X, Yang N, Chen X, Shi S, Shi S, Jin Y. Redundant miR-3077-5p and miR-705 mediate the shift of mesenchymal stem cell lineage commitment to adipocyte in osteoporosis bone marrow. *Cell Death Dis* 2013; **4**: e600 [PMID: [23598412](#) DOI: [10.1038/cddis.2013.130](#)]
- 40 **Nakashima T**, Hayashi M, Takayanagi H. New insights into osteoclastogenic signaling mechanisms. *Trends Endocrinol Metab* 2012; **23**: 582-590 [PMID: [22705116](#) DOI: [10.1016/j.tem.2012.05.005](#)]
- 41 **Tseng W**, Graham LS, Geng Y, Reddy A, Lu J, Effros RB, Demer L, Tintut Y. PKA-induced receptor activator of NF-kappaB ligand (RANKL) expression in vascular cells mediates osteoclastogenesis but not matrix calcification. *J Biol Chem* 2010; **285**: 29925-29931 [PMID: [20663885](#) DOI: [10.1074/jbc.M110.117366](#)]
- 42 **Martin TJ**, Sims NA. RANKL/OPG; Critical role in bone physiology. *Rev Endocr Metab Disord* 2015; **16**: 131-139 [PMID: [25557611](#) DOI: [10.1007/s11154-014-9308-6](#)]
- 43 **Torstrick FB**, Guldberg RE. Local strategies to prevent and treat osteoporosis. *Curr Osteoporos Rep* 2014; **12**: 33-40 [PMID: [24510761](#) DOI: [10.1007/s11914-014-0191-6](#)]
- 44 **Andreopoulou P**, Bockman RS. Management of postmenopausal osteoporosis. *Annu Rev Med* 2015; **66**: 329-342 [PMID: [25386933](#) DOI: [10.1146/annurev-med-070313-022841](#)]
- 45 **Favus MJ**. Bisphosphonates for osteoporosis. *N Engl J Med* 2010; **363**: 2027-2035 [PMID: [21083387](#)]

- DOI: [10.1056/NEJMct1004903](https://doi.org/10.1056/NEJMct1004903)]
- 46 **Khan M**, Cheung AM, Khan AA. Drug-Related Adverse Events of Osteoporosis Therapy. *Endocrinol Metab Clin North Am* 2017; **46**: 181-192 [PMID: [28131131](https://pubmed.ncbi.nlm.nih.gov/28131131/) DOI: [10.1016/j.ecl.2016.09.009](https://doi.org/10.1016/j.ecl.2016.09.009)]
 - 47 **Hu L**, Yin C, Zhao F, Ali A, Ma J, Qian A. Mesenchymal Stem Cells: Cell Fate Decision to Osteoblast or Adipocyte and Application in Osteoporosis Treatment. *Int J Mol Sci* 2018; **19** [PMID: [29370110](https://pubmed.ncbi.nlm.nih.gov/29370110/) DOI: [10.3390/ijms19020360](https://doi.org/10.3390/ijms19020360)]
 - 48 **Tella SH**, Gallagher JC. Prevention and treatment of postmenopausal osteoporosis. *J Steroid Biochem Mol Biol* 2014; **142**: 155-170 [PMID: [24176761](https://pubmed.ncbi.nlm.nih.gov/24176761/) DOI: [10.1016/j.jsbmb.2013.09.008](https://doi.org/10.1016/j.jsbmb.2013.09.008)]
 - 49 **Dempster DW**, Laming CL, Kostenuik PJ, Grauer A. Role of RANK ligand and denosumab, a targeted RANK ligand inhibitor, in bone health and osteoporosis: a review of preclinical and clinical data. *Clin Ther* 2012; **34**: 521-536 [PMID: [22440513](https://pubmed.ncbi.nlm.nih.gov/22440513/) DOI: [10.1016/j.clinthera.2012.02.002](https://doi.org/10.1016/j.clinthera.2012.02.002)]
 - 50 **Muruganandan S**, Roman AA, Sinal CJ. Adipocyte differentiation of bone marrow-derived mesenchymal stem cells: cross talk with the osteoblastogenic program. *Cell Mol Life Sci* 2009; **66**: 236-253 [PMID: [18854943](https://pubmed.ncbi.nlm.nih.gov/18854943/) DOI: [10.1007/s00018-008-8429-z](https://doi.org/10.1007/s00018-008-8429-z)]
 - 51 **Nuttall ME**, Gimble JM. Is there a therapeutic opportunity to either prevent or treat osteopenic disorders by inhibiting marrow adipogenesis? *Bone* 2000; **27**: 177-184 [PMID: [10913909](https://pubmed.ncbi.nlm.nih.gov/10913909/) DOI: [10.1016/s8756-3282\(00\)00317-3](https://doi.org/10.1016/s8756-3282(00)00317-3)]



Published By Baishideng Publishing Group Inc
7041 Koll Center Parkway, Suite 160, Pleasanton, CA 94566, USA
Telephone: +1-925-3991568
E-mail: bpgoffice@wjgnet.com
Help Desk: <https://www.f6publishing.com/helpdesk>
<https://www.wjgnet.com>

